

UC Irvine

UC Irvine Previously Published Works

Title

Systematic assessment of terrestrial biogeochemistry in coupled climate-carbon models

Permalink

<https://escholarship.org/uc/item/9hs5m90v>

Journal

Global Change Biology, 15(10)

ISSN

1354-1013

Authors

Randerson, JT
Hoffman, FM
Thornton, PE
et al.

Publication Date

2009-09-17

DOI

10.1111/j.1365-2486.2009.01912.x

Supplemental Material

<https://escholarship.org/uc/item/9hs5m90v#supplemental>

Copyright Information

This work is made available under the terms of a Creative Commons Attribution License, available at <https://creativecommons.org/licenses/by/4.0/>

Peer reviewed

Systematic assessment of terrestrial biogeochemistry in coupled climate–carbon models

JAMES T. RANDERSON*, FORREST M. HOFFMAN†, PETER E. THORNTON‡§, NATALIE M. MAHOWALD¶, KEITH LINDSAY‡, YEN-HUEI LEE‡, CYNTHIA D. NEVISON*, SCOTT C. DONEY**, GORDON BONAN‡, RETO STÖCKLI††‡, CURTIS COVEY§§, STEVEN W. RUNNING¶¶ and INEZ Y. FUNG|||

*Department of Earth System Science, Croul Hall, University of California, Irvine, CA 92697, USA, †Oak Ridge National Laboratory, Computational Earth Sciences Group, PO Box 2008, Oak Ridge, TN 37831, USA, ‡Climate and Global Dynamics, National Center for Atmospheric Research, PO Box 3000, Boulder, CO 80307, USA, §Oak Ridge National Laboratory, Environmental Sciences Division, PO Box 2008, Oak Ridge, TN 37831, USA, ¶Department of Earth and Atmospheric Sciences, 2140 Snee Hall, Cornell University, Ithaca, NY 14850, USA, ||Institute for Arctic and Alpine Research (INSTAAR), University of Colorado, Boulder, CO 80309, USA, **Department of Marine Chemistry and Geochemistry, MS 25, Woods Hole Oceanographic Institution, Woods Hole, MA 02543, USA, ††Department of Atmospheric Sciences, Colorado State University, Ft Collins, CO 80523, USA, ‡‡MeteoSwiss, Climate Service, Federal Office of Meteorology and Climatology, CH-8044 Zurich, Switzerland, §§Program for Climate Model Diagnosis and Intercomparison, 7000 East Avenue, Bldg. 170, L-103, Livermore, CA 94550-9234, USA, ¶¶Numerical Terradynamic Simulation Group, College of Forestry & Conservation, University of Montana, Missoula, MT 59812, USA, ||||Department of Earth and Planetary Science and Department of Environmental Science, Policy, and Management, 307 McCone, Mail Code 4767, University of California, Berkeley, CA 94720, USA

Abstract

With representation of the global carbon cycle becoming increasingly complex in climate models, it is important to develop ways to quantitatively evaluate model performance against *in situ* and remote sensing observations. Here we present a systematic framework, the Carbon-LAnd Model Intercomparison Project (C-LAMP), for assessing terrestrial biogeochemistry models coupled to climate models using observations that span a wide range of temporal and spatial scales. As an example of the value of such comparisons, we used this framework to evaluate two biogeochemistry models that are integrated within the Community Climate System Model (CCSM) – Carnegie-Ames-Stanford Approach' (CASA') and carbon–nitrogen (CN). Both models underestimated the magnitude of net carbon uptake during the growing season in temperate and boreal forest ecosystems, based on comparison with atmospheric CO₂ measurements and eddy covariance measurements of net ecosystem exchange. Comparison with MODerate Resolution Imaging Spectroradiometer (MODIS) measurements show that this low bias in model fluxes was caused, at least in part, by 1–3 month delays in the timing of maximum leaf area. In the tropics, the models overestimated carbon storage in woody biomass based on comparison with datasets from the Amazon. Reducing this model bias will probably weaken the sensitivity of terrestrial carbon fluxes to both atmospheric CO₂ and climate. Global carbon sinks during the 1990s differed by a factor of two (2.4 Pg C yr⁻¹ for CASA' vs. 1.2 Pg C yr⁻¹ for CN), with fluxes from both models compatible with the atmospheric budget given uncertainties in other terms. The models captured some of the timing of interannual global terrestrial carbon exchange during 1988–2004 based on comparison with atmospheric inversion results from TRANSCOM ($r = 0.66$ for CASA' and $r = 0.73$ for CN). Adding (CASA') or improving (CN) the representation of deforestation fires may further increase agreement with the atmospheric record. Information from C-LAMP has enhanced model performance within CCSM and serves as a benchmark for future development. We propose that an open source, community-wide platform for model-data intercomparison is needed to speed

model development and to strengthen ties between modeling and measurement communities. Important next steps include the design and analysis of land use change simulations (in both uncoupled and coupled modes), and the entrainment of additional ecological and earth system observations. Model results from C-LAMP are publicly available on the Earth System Grid.

Keywords: ameriflux, atmospheric tracer transport model intercomparison project (TRANSCOM), community land model, free air carbon dioxide enrichment (FACE), net primary production (NPP), surface energy exchange

Received 24 September 2008 and accepted 5 December 2008

Introduction

A robust finding of coupled climate–carbon models is that the capacities of the ocean and the terrestrial biosphere to store anthropogenic carbon will weaken in the 21st century from climate warming (Cox *et al.*, 2000; Friedlingstein *et al.*, 2001; Fung *et al.*, 2005; Denman *et al.*, 2007). This positive feedback whereby warming further increases atmospheric CO₂ has important implications for climate mitigation policies designed to stabilize greenhouse gas levels. It implies that to achieve stabilization, trajectories of emissions reductions (e.g., Barker *et al.*, 2007) will, themselves, depend on the amount of future warming. Within terrestrial ecosystems, the reductions in sink capacity with climate warming are caused by at least two classes of feedback mechanisms in current models: slowing of net primary production (NPP) in tropical ecosystems with warming and drying, and secondarily, faster carbon cycling and decomposition of wood, detrital material and soil carbon (Friedlingstein *et al.*, 2006; Matthews *et al.*, 2007). In models with dynamic vegetation decreases in NPP may trigger species redistributions that amplify carbon loss and regional warming (Betts *et al.*, 2004; Cox *et al.*, 2004).

Other factors that affect the strength of the terrestrial biosphere–climate feedback include the climate sensitivity (e.g., the temperature change for a CO₂ doubling) and the sensitivity of terrestrial carbon storage to atmospheric composition changes. Models that store large amounts of carbon on land in response to elevated levels of atmospheric CO₂, for example, have a smaller positive climate–carbon feedback than models with a lower CO₂ storage sensitivity (Friedlingstein *et al.*, 2003; Matthews, 2007). This is because greater terrestrial carbon storage causes CO₂ to accumulate more slowly in the atmosphere, and as a consequence, there is less warming for a given trajectory of anthropogenic emissions. Deforestation, in contrast, works to enhance the climate–carbon feedback because a loss of forest cover reduces the potential of the biosphere to store carbon in woody pools in response to elevated levels of CO₂ (Gitz & Ciais, 2004). Deforestation and land use are coupled

with climate in other ways, including land manager responses to drought (e.g., van der Werf *et al.*, 2008), but parameterizations of this have not been developed yet for global models.

For the first generation of climate–carbon models, the overall sensitivity of the land sink to warming varies by a factor of 7 and the gain of the climate–carbon cycle feedback varies by a factor of 5 (Friedlingstein *et al.*, 2006). While this range includes the climate sensitivities of the parent climate models, their land carbon storage sensitivity (averaging $1.4 \pm 0.5 \text{ Pg C ppm}^{-1} \text{ CO}_2$) varies by a factor of 10 in the absence of climate change (Denman *et al.*, 2007). This range could expand further as new classes of mechanisms are integrated within the models (e.g., Field *et al.*, 2007), including land use (e.g., Hurtt *et al.*, 2006) and climate effects on nitrogen cycling (e.g., Thornton *et al.*, 2007). To reduce this uncertainty and improve the models, comprehensive means are needed for assessing model performance against available observations.

The testing requirements for the land component of coupled climate–carbon models are unique from other types of models such as land surface models (LSMs) or stand-alone terrestrial biogeochemical models for several reasons. First, the biogeochemistry, ecology, and biophysics must be fully integrated. Ecological control of leaf area by carbon and nutrient availability, for example, subsequently influences evapotranspiration and surface energy fluxes that in turn regulate climate and ecosystem dynamics. This contrasts with many (but not all) LSMs that have prescribed leaf area. Second, a key application for these models is to characterize carbon–climate feedbacks from preindustrial times through the end of the 21st century, information that then can be used in the design of realistic emissions scenarios for stabilization. In this context, the models must operate at scales that span minutes to centuries. To capture feedbacks on decadal and centennial time scales, the models must realistically simulate longer lived carbon pools in trees and soils as well as their sensitivity to changes in atmospheric composition and climate. Relevant ecosystem–climate interactions that

shape this sensitivity include physiological and canopy-scale processes such as photosynthesis, decomposition, leaf phenology, and allocation. Of equal importance are processes that often operate on wider spatial and temporal scales such as disturbance, recruitment, mortality, migration, and management. These latter processes play important roles in regulating community composition and diversity and their sensitivity to global change.

Past work to validate coupled climate–carbon models has included comparison with ice core CO₂ observations during the 19th and 20th centuries (Berthelot *et al.*, 2002), the mean annual cycle of atmospheric CO₂ (Doney *et al.*, 2006) and its changing shape (Berthelot *et al.*, 2002), the contemporary carbon budget (Matthews, 2007) and measurements of the sensitivity of NPP to elevated CO₂ from free air carbon dioxide enrichment (FACE) experiments (Matthews, 2007). These tests of coupled models build upon an extensive intercomparison and evaluation history within the terrestrial biogeochemistry and land modeling communities (Schimel *et al.*, 1997; Cramer *et al.*, 2001; McGuire *et al.*, 2001; Dargaville *et al.*, 2002; Morales *et al.*, 2005). However, a systematic framework evaluating the coupled behavior of the land carbon system as well as the interaction between climate and land biogeochemistry has been lacking, and is needed to reduce and assess uncertainties associated with future climate change projections. Such an evaluation is hampered also by the lack of global, multitemporal gridded datasets of terrestrial carbon pools and fluxes, such as National Centers for Environmental Prediction (NCEP) or European Centre for Medium-Range Weather Forecast ERA-40 reanalysis products currently available for atmospheric variables.

Here we present the first part of a systematic framework for evaluating the land component of coupled climate–carbon models, using observations we have compiled that span multiple temporal and spatial scales. We use these observations to evaluate two biogeochemistry models that are coupled to the Community Climate System Model (CCSM) version 3.1 Community Land Model (CLM). The two terrestrial biogeochemical modules are: (1) Carnegie-Ames-Stanford Approach' (CASA'; Fung *et al.*, 2005; Doney *et al.*, 2006) and (2) carbon–nitrogen (CN; Thornton & Zimmermann, 2007; Thornton *et al.*, 2007). In our analysis, we develop a scoring system that weights the information derived from different data streams. We conclude by identifying directions for model improvements and gaps in existing model-data intercomparison systems.

Methods

We first describe CLM, CASA', and CN models. We then describe the model simulation protocols and the

observations that we used to evaluate model performance. In this first phase of the Carbon-LAnd Model Intercomparison Project (C-LAMP), we forced the models in an uncoupled mode with atmospheric reanalysis observations and atmospheric CO₂ and N-deposition trajectories during the 20th century to allow for direct comparison with several different sets of interannually varying observations. In a second (future) phase of C-LAMP we will use partly-coupled models (land component coupled with an interactive atmosphere climate model) to evaluate other aspects of model performance.

Model description

The two biogeochemistry models described below were directly coupled with a modified version of the CLM version 3 (Dickinson *et al.*, 2006). This meant that energy and water exchange and gross primary production (GPP) were estimated by CLM at each time step, providing boundary conditions (including soil moisture and temperature) for the biogeochemistry models. Based on local resource availability and carbon exchange, the biogeochemistry models, in turn, prognostically estimated leaf area that was used by CLM in the following time step. Both biogeochemical models utilize the same plant functional types (PFTs) and their geographical distribution as in CLM, except as noted as follows for CN.

This version of CLM deviates from CLM3 in that canopy leaf area and radiation interception includes explicit treatment of sunlit and shaded canopy fractions, as well as an analytical solution for vertical canopy gradients of specific leaf area (Thornton & Zimmermann, 2007). The photosynthetic parameter V_{cmax} is calculated based on leaf nitrogen concentration and leaf physiological parameters. This canopy integration scheme interacts with the nitrogen cycle in CN, but is unconstrained for nitrogen availability in CASA'. Additionally, vegetation and soil hydrology parameterizations were modified to improve evapotranspiration partitioning and to reduce the dry soil bias in CLM3 (Lawrence *et al.*, 2007). Many of these model changes were implemented in CLM3.5 (Oleson *et al.*, 2008). CN additionally has unique hydrological parameterizations that differ from CLM. CLM was configured to run with a 20-min time step using a standard T42 Gaussian grid with a resolution of approximately $2.8^\circ \times 2.8^\circ$.

CASA'

CASA' is derived from the off-line land biogeochemistry model CASA (Potter *et al.*, 1993; Randerson *et al.*, 1997) and tracks the flow of carbon through live vegetation, litter, and soil organic matter pools. A primary

difference between the two models is that CASA estimates monthly NPP from satellite observations of the fraction of absorbed photosynthetically active radiation (fAPAR), while CASA' assumes NPP is 50% of the instantaneous GPP calculated from CLM. CASA' was used by Fung *et al.* (2005) to examine feedbacks during the 21st century and by Doney *et al.* (2006) to explore the dynamics of global climate–carbon cycle interactions during a period without anthropogenic forcing.

In CASA', allocation of NPP to leaves, wood, and fine roots depends on water availability and light limitation following Friedlingstein *et al.* (1999). Leaf area is then determined from the leaf carbon and specific leaf area estimates described by Dickinson *et al.* (1998). Mortality rates of leaves, wood, and fine roots are PFT dependent and generate a flow of carbon into leaf, coarse woody debris, and fine root litter pools. Heterotrophic respiration and carbon flow in litter and soil organic matter pools vary with soil temperature and moisture and tissue chemistry. Altogether there are three living and nine dead carbon pools, including four soil organic matter pools that represent soil carbon fractions with turnover times ranging from months to centuries. A more detailed description of the model is provided by Doney *et al.* (2006).

CN

CN is the result of merging the biophysical framework of CLM with the fully prognostic carbon and nitrogen dynamics of the terrestrial biogeochemistry model Biome-BGC (version 4.1.2) (Thornton *et al.*, 2002, Thornton & Rosenbloom, 2005). The resulting model (Thornton *et al.*, 2007) is fully prognostic with respect to all carbon and nitrogen state variables in vegetation, litter, and soil organic matter, and retains all prognostic quantities for water and energy in the vegetation–snow–soil column from CLM. Vegetation pools include leaf, respiring and nonrespiring woody components of stem and coarse roots, and fine roots. Plant storage pools allow carbon and nitrogen acquired in one growing season to be retained and then distributed as new growth in subsequent years. Prognostic leaf phenology is based on classification of PFTs as evergreen, seasonal deciduous, or stress-deciduous, while prognostic leaf area index (LAI) is based on the prognostic leaf carbon pool and an assumed vertical gradients of specific leaf area (Thornton & Zimmermann, 2007). The heterotrophic model includes carbon and nitrogen storage and fluxes for a coarse woody debris pool, three litter pools and four soil organic matter pools, arranged as a converging trophic cascade (Thornton *et al.*, 2005). A prognostic treatment of fire is included based on the

model of Thonicke *et al.* (2001). Detailed descriptions for all biogeochemical components of CN, and for those aspects of the biophysical framework modified to accommodate prognostic vegetation structure, are given in Thornton *et al.* (2007).

CN uses the same PFTs as CLM except that it excludes temperate broadleaf deciduous trees from tropical regions and reclassifies these as tropical deciduous trees. CN also removes the exponential decline in rooting distribution with depth used in CLM, replacing this with a linearly decreasing rooting distribution that has a shallower bottom rooting depth for grasses than for shrubs and trees.

Model simulations

In the set of experiments presented here we forced the models with an improved NCAR/NCEP atmospheric reanalysis dataset in which temperature and precipitation values were adjusted using monthly mean gridded observations (Qian *et al.*, 2006). The goal of these uncoupled simulations was to allow for direct comparison with interannually varying observations obtained during the last few decades. Model simulations are summarized in Table 1. Both models were spun up for approximately 4000 years forced with repeated cycling of the first 25 years of the reanalysis climate (1948–1972) and fixed, preindustrial atmospheric CO₂. The initial 500-year phase of the CN model spin-up employed an accelerated decomposition technique (Thornton & Rosenbloom, 2005). At the end of model spin up (experiment 1.1), a control simulation (experiment 1.2) was performed for the period 1798–2004 using the same repeating 25-year reanalysis climate forcing. A varying climate simulation (experiment 1.3), branched from the control in year 1948 and was forced by the full reana-

Table 1 Model simulations performed in C-LAMP phase 1

Run	Description	Time period
<i>Forcing with observed climate</i>		
1.1	Spin-up	~ 4000 years
1.2	Control	1798–2004
1.3	Varying climate	1948–2004
1.4	Varying climate, CO ₂ , and N deposition	1798–2004
<i>FACE simulations</i>		
1.5	Control – CO ₂ levels and N deposition after 2004 held constant	1997–2010
1.6	Branch from Experiment 1.4 in 1997 to CO ₂ at 550 ppm	1997–2010

C-LAMP, Carbon-LAnd Model Intercomparison Project.

lysis time series from 1948 to 2004. Both experiments 1.2 and 1.3 also had fixed, preindustrial atmospheric CO₂. A second transient simulation (experiment 1.4) started from the end of model spin up and ran for the period 1798–2004. This simulation had a prescribed, time-varying atmospheric CO₂ time series starting in 1798. For CN, a nitrogen deposition climatology was used as a model driver before 1890 followed by a prescribed nitrogen deposition time series from 1890 to 2004. Climate forcing in experiment 1.4 was the same as the control from 1798 to 1947 and as experiment 1.3 from 1948 to 2004. No land use change or dynamic vegetation simulations were included in this first C-LAMP analysis: land cover was prescribed with preindustrial (year 1798) distributions using the dataset developed by Feddema *et al.* (2005). This was done so that future C-LAMP simulations could branch from this point with transient land cover change.

The prescribed global atmospheric CO₂ time series was from the C⁴MIP reconstruction from Friedlingstein *et al.* (2006), extended through 2004. The nitrogen deposition climatology and 1890–2004 time series were developed as part of the SANTA FE project (Lamarque *et al.*, 2005). Two additional simulations (experiments 1.5 and 1.6) were designed to test the response of the models to a sudden increase in atmospheric CO₂, following a protocol similar to FACE experiments. These two latter experiments branched from experiment 1.4 in 1997, with CO₂ levels abruptly increasing from 362 to 550 ppm in experiment 1.6. In experiment 1.5, CO₂ levels followed atmospheric observations from 1997 to 2004 and then remained constant thereafter at 379.1 ppm. We extended these two simulations to 2010 to explore carbon sink dynamics during the time of ongoing FACE experiments. More detailed information about the spin up and simulation protocol is available in Hoffman *et al.* (2008) and at <http://www.climate modeling.org/c-lamp/protocol/protocol.html>.

Metadata standards for terrestrial biosphere model output were developed as part of the C-LAMP protocol. Proposed as extensions to the netCDF Climate and Forecast (CF) conventions (Eaton *et al.*, 2008), these naming conventions will be needed to support output of model results coming from earth system models performing simulations for the Intergovernmental Panel on Climate Change (IPCC) Fifth Assessment Report (AR5). The proposed extensions are described at http://www.climate modeling.org/c-lamp/protocol/model_output.php. Model results from C-LAMP are publicly available through the Earth System Grid Center for Enabling Technologies (ESG-CET; Ananthakrishnan *et al.*, 2007) under the same terms as the database of physical climate model output used in the IPCC AR4 (Meehl *et al.*, 2007). The Earth System Grid (ESG;

<http://www.earthsystemgrid.org/>) is a distributed system that allows registered users to download model output, code, and ancillary data over the Internet (Bernholdt *et al.*, 2005). A new ESG node has been deployed at ORNL to support C-LAMP.

Metrics

Multiple sets of observations exist for evaluating terrestrial biogeochemistry model performance on a range of temporal and spatial scales (supporting information Fig. S1). Combining information from these different data streams to evaluate model performance requires consideration of the primary objective(s) of the model simulations, an understanding of the uncertainties associated with each type of observation, and the degree to which scaling issues influence the comparison. We describe below the different observations used in our analysis.

Leaf area

We compared model estimates with MODerate Resolution Imaging Spectroradiometer (MODIS) LAI observations (MOD15A2 collection 4; Myneni *et al.*, 2002) with additional adjustments to interpolate across periods of cloud contamination as described by Zhao *et al.* (2005). We specifically evaluated the models against three aspects of the observations: the timing or phase of maximum LAI (as a diagnostic of seasonality), maximum monthly LAI, and annual mean LAI. For the mean and maximum, biases may exist in the satellite-derived estimates from errors in atmospheric and canopy radiative transfer models used in the retrieval. The metric of the seasonality, based on the month of maximum LAI, should be less sensitive to these types of biases, and thus probably has a lower overall level of uncertainty. In our analysis, we compared 2000–2004 monthly mean MODIS values with model estimates from experiment 1.4 sampled during the same time period.

In climate–carbon models, leaf area is a key prognostic variable that couples biophysics, hydrology, and biogeochemistry. To account for different levels of uncertainty in our scoring system we gave more weight to the comparison of LAI phase than to the maximum or mean. For the phase, we computed the temporal offset (in months) between model and observations in each cell, normalized this amount by a maximum possible offset (6 months), and then averaged this quantity for all the grid cells in each biome. A quantitative description of this metric and our scoring approach for LAI is provided in the supporting information [including Eqn (s1)]. For the maximum and annual mean LAI

comparisons, we estimated the absolute difference between the model and satellite observations at each grid cell, normalized this quantity by the sum of model and observations, and then averaged this quantity for all the grid cells in a biome [Eqn (s2) in the supporting information].

NPP

Even though considerable uncertainty exists with field-based measurement approaches, we included NPP as one of our metrics because it is a fundamental quantity that determines the availability of food, fuel, and fiber resources for humans. It also regulates carbon storage in long-lived pools (such as wood) that, in turn, determines the magnitude of terrestrial sinks and sources in response to various drivers of global change. We used two data sources for our comparisons: compilations of NPP observations from the Ecosystem Model Data Intercomparison (EMDI) (Olson *et al.*, 2001) and spatial patterns of NPP derived using MODIS satellite observations (Zhao *et al.*, 2005, 2006). To extract information from these two datasets, we designed four different comparisons. Using the EMDI observations, we made (1) point-by-point comparisons of observations and corresponding model grid cells and (2) histograms of NPP vs. precipitation for both the observations and the models. We evaluated model performance using Eqn (s2) in the supporting information in grid cells where EMDI observations were available. Separate comparisons were made for EMDI observations classified as high quality (81 sites; class A) and intermediate quality (933 sites; class B). NPP observations were compared with mean annual NPP averaged during 1975–2000 from experiment 1.4.

A large mismatch in spatial scale between the site-level EMDI observations and the size of an individual model grid cell probably compromises the value of this dataset for evaluating model performance. In contrast, MODIS NPP estimates are based on high resolution (1 km) satellite measurements of the fAPAR across the entire domain of a model grid cell, potentially limiting errors associated with scaling. Here we used the MOD17A3 collection 4.5 product (Heinsch *et al.*, 2003). Biases could exist, however, in MODIS NPP if there are errors associated with the underlying algorithms that convert satellite radiances to fAPAR or with the conversion of APAR to NPP using a light use efficiency model. To try to avoid these biases in our scoring system (but still maintaining access to the rich spatial information from the satellite observations), we computed the square of the Pearson correlation coefficient (r^2) between MODIS NPP and the models using all

model grid cells and, separately, using the latitudinal zonal means.

The annual cycle of atmospheric carbon dioxide

Measurements of the annual cycle of atmospheric CO₂ from NOAA's Global Monitoring Division (GMD) and other networks (Globalview; Masarie & Tans, 1995) provide a means to evaluate model fluxes of monthly NEE for biomes in the northern part of the northern hemisphere. Seasonal NEE fluxes are controlled by both the magnitude and timing of NPP and the temperature sensitivity of heterotrophic respiration (Kaminski *et al.*, 2002; Randerson *et al.*, 2002). Measurements of the annual cycle are a robust constraint at a large spatial scale on the combined set of processes regulating NEE because (1) ocean and fossil fuel fluxes contribute only weakly to seasonal variations in CO₂ in the northern hemisphere (Randerson *et al.*, 1997; Heimann *et al.*, 1998; Nevison *et al.*, 2008) and (2) the CO₂ measurements are precise (Conway *et al.*, 1994). These data-model comparisons are sensitive, however, to biases in the atmospheric model—particularly with respect to convection, planetary boundary layer mixing, and other processes that regulate vertical mixing (Stephens *et al.*, 2007; Yang *et al.*, 2007).

To compare with the Globalview observations, we combined CASA' and CN surface CO₂ fluxes with monthly atmospheric impulse functions from the Atmospheric Tracer Transport Model Intercomparison Project (TRANSCOM) phase 3 level 2 experiments (Gurney *et al.*, 2004) to construct simulated annual cycles of atmospheric CO₂. Using techniques applied in interannual inversions, the response functions were used to fill a matrix (the H matrix defined in Baker *et al.*, 2006). Monthly NEE fluxes from CASA' and CN 1.4 experiments for 1988–2000 were aggregated within each of the 11 TRANSCOM land basis regions. The aggregated fluxes were multiplied by the H matrix to construct modeled 1991–2000 interannual CO₂ mixing time series at observation stations. We computed an annual cycle for each of the 13 TRANSCOM atmospheric models and report the model mean. For our scoring system, we estimated model performance in three different latitude bands in the northern hemisphere. We computed the square of the Pearson correlation coefficient (as a metric of phase) and the ratio of model to observed amplitudes (as a metric of magnitude) for each Globalview station. Each station was weighted equally in constructing the zonal means. We assigned a higher number of possible points to the 90–60°N and 30–60°N latitude zones than to the EQ – 30°N band because the signal to noise ratio of the observed annual cycle is higher at mid and high latitudes and because

the contribution in these bands from other fluxes (from ocean and fossil fuel fluxes) is substantially lower.

Eddy covariance measurements of energy and carbon

Eddy covariance measurements provide a powerful constraint on surface energy exchange (Stockli *et al.*, 2008), the seasonal dynamics of NEE (Falge *et al.*, 2002) and GPP (Falge *et al.*, 2002; Heinsch *et al.*, 2006). Prognostic leaf area from the biogeochemical model must be integrated with other aspects of the LSM to predict, for example, the flow of available energy into latent and sensible heat. Here we compared the models with available gap-filled Ameriflux level 4 data (<http://public.ornl.gov/ameriflux/available.shtml>). We made specific comparisons against monthly mean fluxes of (1) NEE, (2) GPP, (3) latent heat, and (4) sensible heat. We sampled the model grid cells (from experiment 1.4) during each year that the observations were available to build a multiyear set of mean monthly fluxes through 2004. We estimated model-data agreement using Eqn (s2) in the supporting information at each site using the monthly means, and weighted information from each site equally in constructing our overall score. We assigned fewer scoring points to the GPP and NEE comparisons based on a subjective assessment that these fluxes had higher measurement and scaling uncertainties, respectively, than concurrent latent and sensible heat fluxes (see text in supporting information).

We present specific site-level comparisons for Sylvia Wilderness (Desai *et al.*, 2005), Harvard Forest (Barford *et al.*, 2001), and Walker Branch (Wilson & Baldocchi, 2001). For our overall scoring system, however, we used information for each variable from all available Ameriflux sites. This included information from 74 sites, ranging from arctic tundra at Atkasuk (70°N) to pine forests at the Kennedy Space Center (28°N). A primary source of uncertainty in the model-data comparison for eddy covariance observations is the spatial scale mismatch. This may be improved in future by forcing the models directly with site-level climate observations and with PFT distributions that match the observed distribution within the tower footprint (e.g., Stockli *et al.*, 2008).

Aboveground biomass stocks and fluxes

Aboveground carbon in contemporary forests is a large and vulnerable carbon pool that is sensitive to both land use and climate change. The size of this pool is one of the primary uncertainties associated with estimates of contemporary carbon loss from deforestation. Within the Amazon basin, considerable effort has gone into developing methods to measure and extrapolate forest

biomass to basin-wide inventories (Fearnside, 1992; Houghton *et al.*, 2001). In Brazil's Amazonian forests, estimates of total live and dead biomass (including coarse roots) range between 39 and 93 Pg C, with a mean and standard error of 70 ± 8 Pg C (Houghton *et al.*, 2001). To compare with model estimates, we used the map of contemporary (ca. 2000) aboveground live biomass developed by Saatchi *et al.* (2007). This map was developed using 540 plot measurements of biomass, including the 44 measurements summarized by Houghton *et al.* (2001), and a decision tree classification approach based on multiple satellite data sets. Within the Amazon basin, mean forest biomass (including live, dead, and belowground wood) was 158 Mg C ha^{-1} for a total of 86 Pg C within the study domain of $5.46 \times 10^6 \text{ km}^2$ (Saatchi *et al.*, 2007). For our scoring metric we used Eqn (s2) in the supporting information. We specifically compared model output for the year 2000 from experiment 1.4 with the observations at each grid cell.

Sensitivity of NPP to increasing levels of atmospheric CO₂

To characterize the sensitivity of model NPP to elevated levels of CO₂ we performed two model simulations described above (experiments 1.5 and 1.6) to mimic control and treatment plots in FACE experiments. We made a direct comparison of temperate forest grid cell NPP increases with site level averages from Norby *et al.* (2005) – estimating the percent increases in NPP separately for grid cells corresponding to each of the four FACE sites. The model-data differences for the four sites were used with Eqn (s2) in the supporting information to generate a scoring metric. We also report the zonal mean responses of the two models.

We computed the biotic growth factor, β_{fert} , as:

$$\beta_{\text{fert}} = \frac{(NPP_f - NPP_i)/NPP_i}{\ln(C_f/C_i)} \quad (1)$$

where NPP_i was the mean NPP from the control during 1997–2001 (exp. 1.5) and NPP_f was the mean NPP from the FACE simulation (exp. 1.6) for this same period. C_i and C_f were the control (~ 365 ppm) and FACE (550 ppm) atmospheric CO₂ mixing ratios.

Interannual variability in carbon fluxes

We compared model estimates of interannual variability in NEE with flux estimates from TRANSCOM (Baker *et al.*, 2006). The TRANSCOM fluxes were obtained using Globalview CO₂ measurements and the same impulse–response functions described above. The inversion was based on observations from 78 flask

stations and a Bayesian approach with seasonally varying *a priori* uncertainties for land regions, time-invariant prior uncertainties for the ocean, and a diagonal error covariance matrix which was comprised of the variance of the observations measured at each station. Fluxes from Baker *et al.* (2006) spanned the 1988–2003 period. For comparison with C-LAMP models, they were extended by Baker through 2004 using the same station network and inversion approach (D. Baker, personal communication, March 2008). Our scoring metric combined information about (1) the correlation between the global annual mean model fluxes and the observations during 1988–2004 and (2) the magnitude of model variability as compared with that in the observations.

Fire emissions were assessed by comparing CN with the Global Fire Emissions Database version 2 (GFEDv2) (van der Werf *et al.*, 2006). The version of CASA' evaluated here did not predict fires. GFEDv2 estimates of burned area were constructed by combining MODIS active fire observations with MODIS burned area tiles (where available) using a regression tree approach (Giglio *et al.*, 2006). We used Eqn (s2) in the supporting information with globally averaged monthly fluxes during 1997–2004 to estimate model performance.

We note that both the TRANSCOM and GFEDv2 fluxes were obtained using models as key intermediary steps in transforming raw observations to fluxes. Uncertainties in these models – including biases in atmospheric transport for TRANSCOM and biases in fuel loads and combustion completeness for GFEDv2 are difficult to quantify. As a result, the total number of points we assigned to these comparisons in our scoring system was lower than for other classes of constraints in the transient dynamics section. We expect the quality of both these time series to improve in future with new satellite observations (e.g., Crisp *et al.*, 2004) and data assimilation systems.

Results

Comparison with MODIS LAI showed that for both models, the timing of maximum leaf area lagged behind the observations by 1–2 months (Fig. 1). In many boreal and arctic ecosystems, for example, maximum observed LAI occurred in July, whereas in the models the maximum occurred in August (CASA') or September (CN). These lags also occurred in moisture-limited savanna ecosystems, although CN matched observed patterns reasonably well in southern hemisphere South America and CASA' performed reasonably well in Africa. The systematic nature of these timing delays suggests that the prognostic leaf area schemes for both models may underestimate carryover pools of carbohydrates from one growing season to the next – and thus the potential

for rapid leaf expansion at the onset of the growing season. For other aspects of LAI, including mean and maximum levels, the models performed reasonably well in most biomes (data not shown). One exception was that LAI was low in CN in many boreal and arctic regions. This bias was partly a consequence of the coupling to the hydrology model that did not adequately capture freeze-thaw dynamics (Lawrence *et al.*, 2007).

Direct comparison with EMDI site-level NPP showed that CASA' was higher than the observations in intermediate and high productivity areas, whereas CN was lower than the observations in low productivity areas (supporting information Fig. S2). This pattern of bias remained the same when the models were compared as a function of precipitation level (Fig. 2) and latitude (supporting information Fig. S3). Specifically, CASA' had a high bias in high precipitation and tropical areas, whereas CN had a low bias of similar relative magnitude in boreal and arctic ecosystems.

Both models substantially underestimated the seasonal amplitude of CO₂ in the northern hemisphere – CASA' by a factor of ~2 and CN by a factor ~3 (Table 2). CN also had a phase offset with the observations, with drawdown of CO₂ in spring occurring 1–3 months earlier than in the observations (Fig. 3). For CASA' the smaller amplitude was probably caused by either a temperature sensitivity of heterotrophic respiration (e.g., a Q_{10} factor) that was too high in northern ecosystems or a seasonal distribution of NPP that was not concentrated enough during the middle part of the growing season. In contrast, for CN the low NPP in ecosystems north of 40°N (supporting information Fig. S3) also reduced the magnitude of heterotrophic respiration and thus the magnitude of seasonal variations in NEP.

Seasonal variations in NEE were substantially smaller in the models than in the Ameriflux observations (Fig. 4) and are consistent with the model biases described above for the annual cycle of CO₂. One important contributor to this bias was that in both models, the growing season for GPP was too long in temperate forest ecosystems – starting earlier in the spring and extending later in the fall than in the observations. The models also generally under predicted the rate of GPP increase at the onset of the growing season, including at three sites shown in Fig. 4 and at Lost Creek (46°N), Park Falls (46°N), Toledo (42°N), Niwot Ridge (40°N), and Missouri Ozark (39°N) sites (data not shown).

In terms of energy exchange, the models captured patterns of latent heat more accurately than fluxes of sensible heat, with mean scores of 0.71 and 0.52 for CN and 0.71 and 0.54 for CASA' [using Eqn (s2) in the supporting information averaged across all L4 Ameriflux sites]. A large model bias was underestimation of

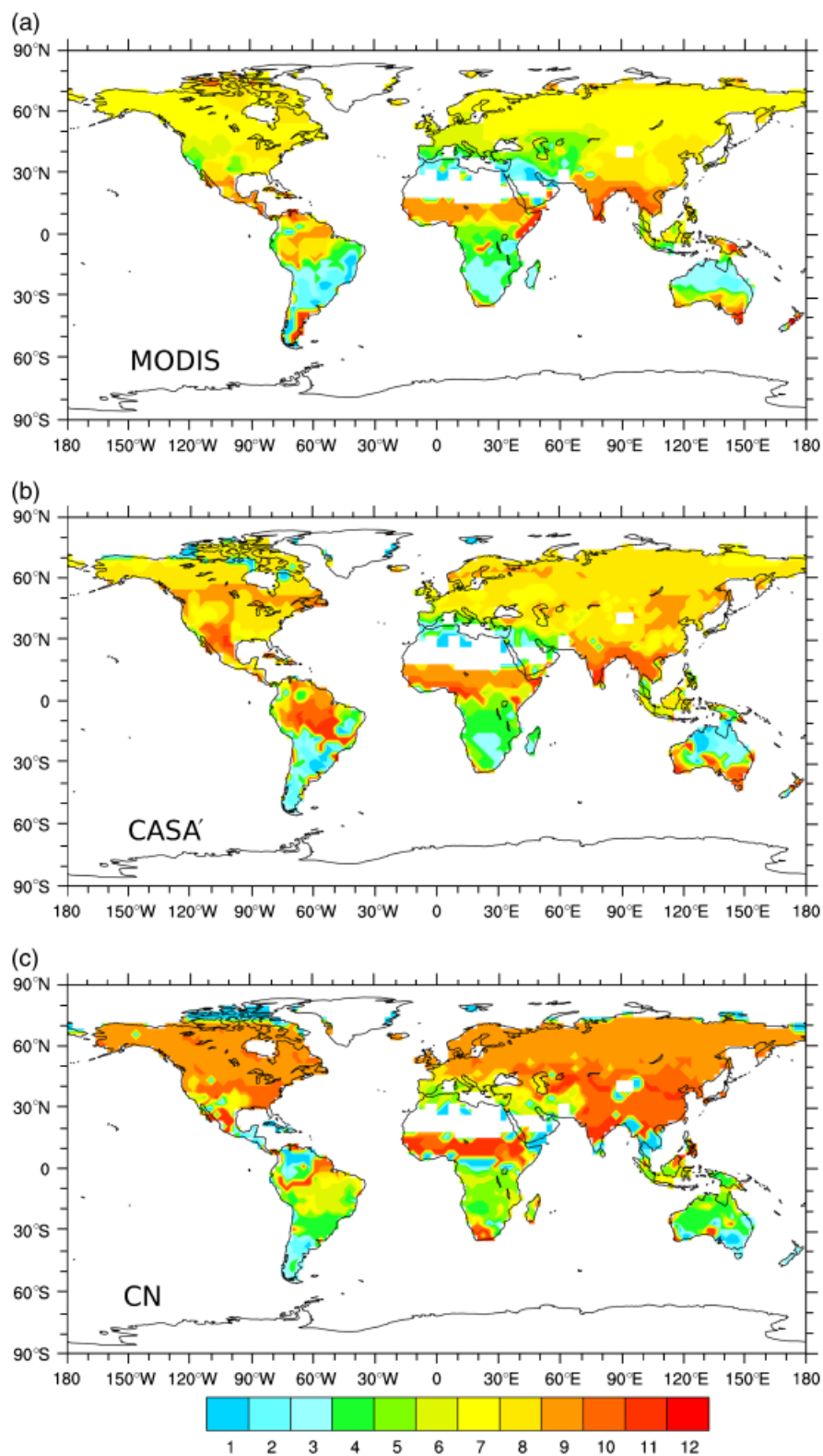


Fig. 1 Month of maximum leaf area index from (a) MODIS, (b) CASA', and (c) CN. The observations are from the MOD15A2 collection 4 LAI product from MODIS (Myneni *et al.*, 2002) with additional adjustments to interpolate across periods of cloud contamination as described by Zhao *et al.* (2005). CASA, Carnegie-Ames-Stanford Approach; CN, carbon-nitrogen; LAI, leaf area index; MODIS, MODerate Resolution Imaging Spectroradiometer.

sensible heat fluxes during winter and spring in temperate and boreal ecosystems. Solar radiation estimates from the reanalysis product used to drive the models (Qian *et al.*, 2006) agreed reasonably well with site-level observations, with a score of 0.93 when averaged across all Ameriflux sites. This implies that incoming short-wave (and cloudiness) was not the primary reason for the model bias. Further diagnosis will require additional net radiation and albedo observations. These variables are not currently available for the publicly available level 4 gap-filled product.

Within the Amazon basin, both models substantially overestimated aboveground live biomass (Fig. 5). The basin-wide total from Saatchi *et al.* (2007) was 69 PgC compared with 199 PgC for CASA' and 161 PgC for CN. Even though the models had a substantial bias in magnitude, they both reproduced the spatial pattern in South America reasonably well ($r = 0.96$ for CASA' and $r = 0.86$ for CN). Some, but certainly not all, of the

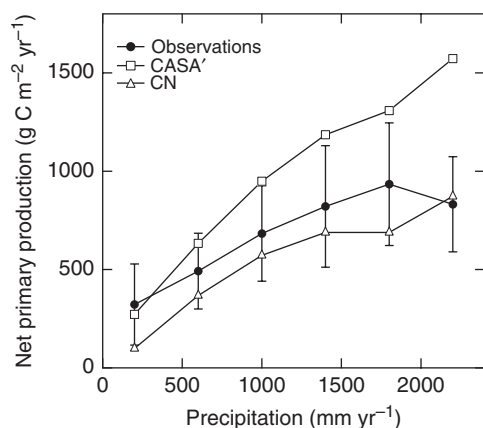


Fig. 2 Net primary production normalized by precipitation for the EMDI NPP observations and the models. The 933 sites from the class B NPP dataset are shown. Site-level annual precipitation from the EMDI dataset was used to construct the histogram for the observations (with 400 mm yr⁻¹ increment bins). For the models, we used precipitation from the climate forcing dataset from Qian *et al.* (2006). EMDI, Ecosystem Model Data Intercomparison Initiative; NPP, net primary production.

positive bias in the basin-wide total in the models, can be attributed to high levels of biomass on the perimeter of the basin (particularly in the south) that resulted from our use of a preindustrial land cover map that had higher fractions of forest cover than what was observed circa 2000 (the time period of the map from Saatchi *et al.*, 2007).

To further assess the causes of this model bias in the tropical forest aboveground live biomass pool, we compared the models with carbon budget observations from Amazonia (Miller *et al.*, 2004; Vieira *et al.*, 2004; Figueira *et al.*, 2008; Malhi *et al.*, 2009). GPP in both CASA' (3220 g C m⁻² yr⁻¹) and CN (2900 g C m⁻² yr⁻¹) was similar to observed levels (3330 ± 420 g C m⁻² yr⁻¹) (Figueira *et al.*, 2008; Malhi *et al.*, 2009). A primary cause of the excess woody biomass in CASA' was that the flow of GPP to autotrophic respiration was too low. In CASA', autotrophic respiration was prescribed at 50% of GPP whereas the mean of observations from Malhi *et al.* (2009) show that 65 ± 10% of GPP was respired in three mature tropical forest ecosystems (Fig. 6). Another contributing factor was that in both models NPP allocation to wood was too high, with levels of 810 g C m⁻² yr⁻¹ and 540 g C m⁻² yr⁻¹, respectively, for CASA' and CN compared to 470 ± 100 g C m⁻² yr⁻¹ for the mean of the three sites reported by Malhi *et al.* (2009). Wood turnover times agree reasonably well with observed pools and fluxes: 37 and 44 years in CASA' and CN compared with a mean of 40 years from Malhi *et al.* (2009). Other studies report even lower wood NPP fluxes (at approximately 200 g C m⁻² yr⁻¹), however, implying that the turnover time of aboveground live biomass is approximately 90 years (assuming the same pool size) (Vieira *et al.*, 2004; Figueira *et al.*, 2008).

In response to an instantaneous increase in CO₂ mixing ratio to 550 ppm in 1997, both models exhibited a positive step change in NPP, with CASA' increasing globally by 17% and CN by 10% during the first 5 years after CO₂ enrichment (Fig. 7). Carbon uptake by the models, in turn, showed a rapid response with CASA' increasing to 12.5 Pg C yr⁻¹ and CN to 4.2 Pg C yr⁻¹ in the first year. The disproportionately large NEE re-

Table 2 Model estimates of the annual cycle of atmospheric CO₂

Latitude Zone	Number of obs. stations	Globalview (GV) seasonal amplitude (ppm)	CASA'		CN	
			Correlation w/GV (r)	Amp. Ratio: CASA'/GV	Correlation w/GV (r)	Amp. Ratio: CN/GV
60–90°N	7	14.6 ± 0.5	0.97 ± 0.02	0.43 ± 0.02	0.77 ± 0.06	0.33 ± 0.02
30–60°N	28	12.9 ± 4.9	0.96 ± 0.03	0.49 ± 0.14	0.84 ± 0.07	0.37 ± 0.13
0–30°N	11	7.0 ± 1.5	0.96 ± 0.08	0.46 ± 0.04	0.91 ± 0.06	0.31 ± 0.03

CASA, Carnegie-Ames Stanford Approach; CN, Carbon-nitrogen; GV, Globalview observations.

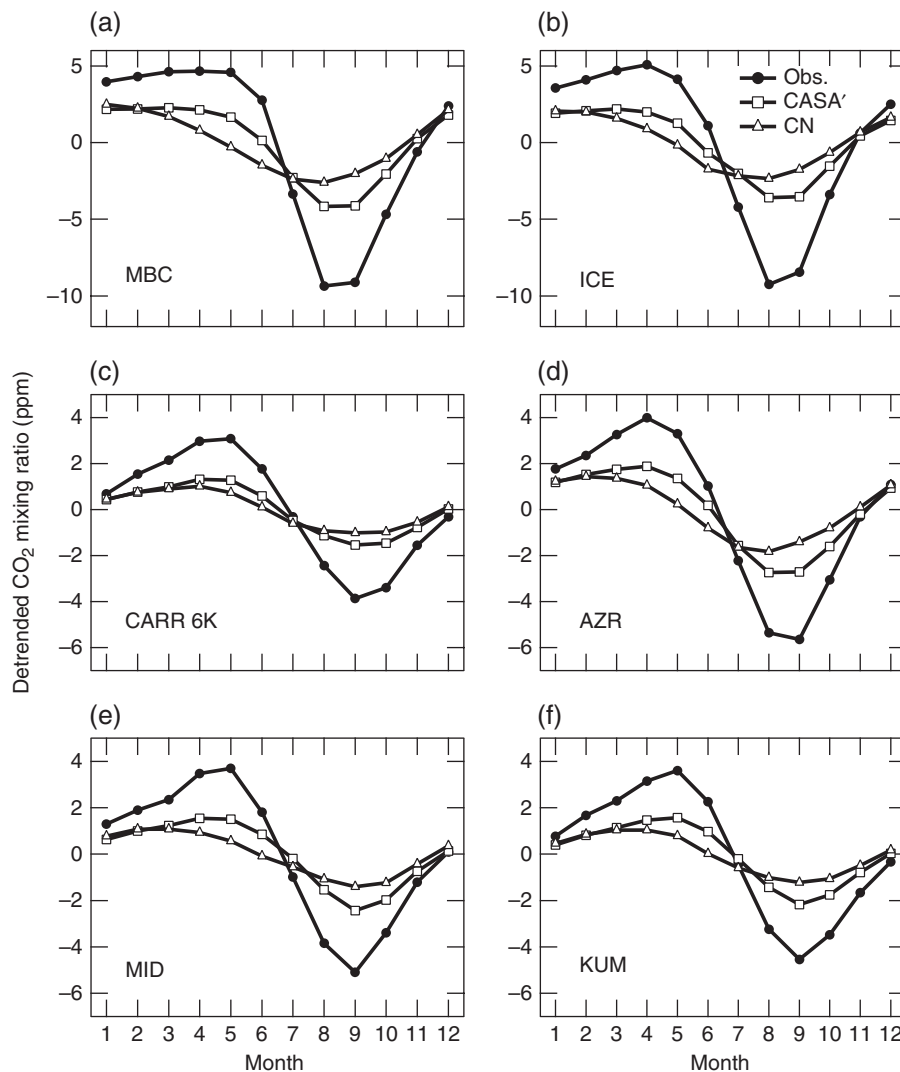


Fig. 3 The annual cycle of atmospheric carbon dioxide at (a) Mould Bay, Canada (76°N), (b) Storhofdi, Iceland (63°N), (c) Carr, Colorado (aircraft samples from 6 km masl; 41°N), (d) Azores Islands (39°N), (e) Sand Island, Midway (28°N), and (f) Kumakahi, Hawaii (20°N). The observations are from Globalview (Masarie & Tans, 1995). The model estimates were obtained using model fluxes from experiment 1.4 and monthly impulse response functions from the TRANSCOM experiment (Gurney *et al.*, 2004). The TRANSCOM multimodel mean estimate is shown for each case.

sponse in CASA' (almost threefold larger than CN) can only be partly attributed to the higher sensitivity of NPP to CO₂ enrichment; other important factors included a higher baseline NPP and similar turnover times in pools involved with initial carbon storage.

At the four model grid cells corresponding to the FACE experiments analyzed by Norby *et al.* (2005), CASA' and CN had NPP increases of $17 \pm 2\%$ ($\beta_{\text{fert}} = 0.43 \pm 0.04$) and $7 \pm 3\%$ ($\beta_{\text{fert}} = 0.18 \pm 0.09$) during the first 5 years, respectively, compared with an observed increase of $27 \pm 2\%$ ($\beta_{\text{fert}} = 0.67$). Both models showed a decreasing trend in NPP response between 40°N and 70°N (supporting information Fig. S4) which

is consistent with decreasing temperatures limiting the role of elevated CO₂ in suppressing photorespiration (Hickler *et al.*, 2008). In arid regions in western North America and central Asia NPP in CASA' had a much larger response than CN, including a 28% increase in broadleaf deciduous temperate shrubs vs. a 12% increase in CN. This suggests that increases in water use efficiency may be a more important factor in shaping the overall response in CASA' than in CN (and as compared with the LPJ-GUESS as analyzed by Hickler *et al.*, 2008). The different spatial patterns in the two models are mostly unconstrained by existing observations and further highlight the need for future FACE

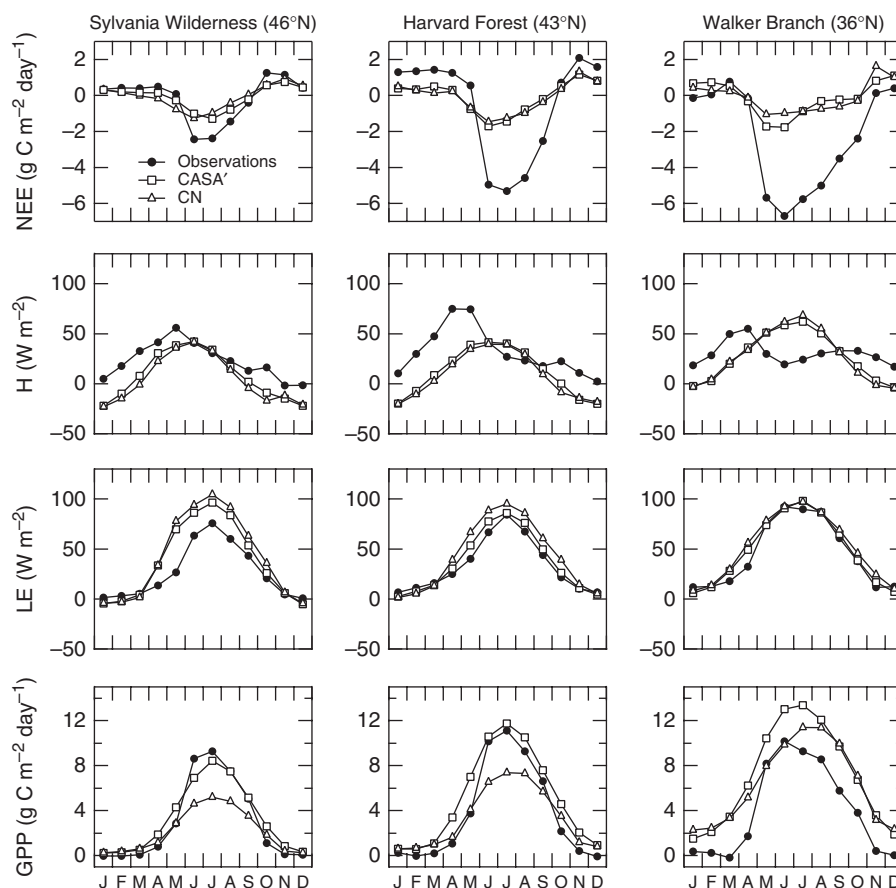


Fig. 4 Comparison of model estimates with eddy covariance measurements from Sylvania Wilderness (Desai *et al.*, 2005), Harvard Forest (Barford *et al.*, 2001), and Walker Branch (Wilson & Baldocchi, 2001) sites from the Ameriflux network. Level 4 gap-filled measurements from all available years were used to construct monthly means. Model information was extracted from experiment 1.4 for the same periods.

experiments that span a much broader range of biomes and climate (Hickler *et al.*, 2008).

Climate variability from the NCAR/NCEP driver dataset led to substantial interannual variability in carbon exchange, with a standard deviation of 1.1 Pg C yr^{-1} for CASA' and 0.8 Pg C yr^{-1} for CN during 1991–2000 (supporting information Fig. S5a). Although the two models had carbon sinks that differed by a factor of 2 during 1991–2000 ($-2.4 \text{ Pg C yr}^{-1}$ for CASA' and $-1.2 \text{ Pg C yr}^{-1}$ for CN), both estimates are compatible with our understanding of the contemporary carbon cycle given uncertainties associated with the size of the deforestation flux and ocean exchange (Denman *et al.*, 2007). Assuming, specifically, that the sum of land and ocean sinks was 3.0 Pg C yr^{-1} during the 1990s, CASA' was compatible with a larger deforestation flux (for example, 1.2 Pg C yr^{-1}) and smaller ocean sink (e.g., 1.8 Pg C yr^{-1}), whereas CN was compatible with a smaller deforestation flux (e.g., 0.6 Pg C yr^{-1}) and a larger ocean flux (e.g., 2.4 Pg C yr^{-1}). In the absence of

climate warming during 1948–2004, contemporary carbon sinks in the two models would have been even larger: a mean of $-2.7 \text{ Pg C yr}^{-1}$ for CASA' and $-1.8 \text{ Pg C yr}^{-1}$ for CN during 1991–2000 (supporting information Fig. S5b). Climate changes alone, including a warming trend on land from the 1970s to 1990s, caused the net flux in both models to change from a sink to a source (supporting information Fig. S5c).

Both models captured some of the interannual variability in land fluxes during 1988–2004 based on comparison with TRANSCOM-derived estimates (Fig. 8). The largest positive anomaly for both the TRANSCOM estimates and the models occurred during the 1998 El Niño. The models were significantly correlated ($P < 0.01$) with TRANSCOM anomalies ($r = 0.66$ for CASA' and $r = 0.73$ for CN) and had year-to-year variability that was similar in magnitude to the observations (1.0 Pg C yr^{-1} standard deviation for CASA', 0.7 Pg C yr^{-1} for CN, and 1.0 Pg C yr^{-1} for TRANSCOM).

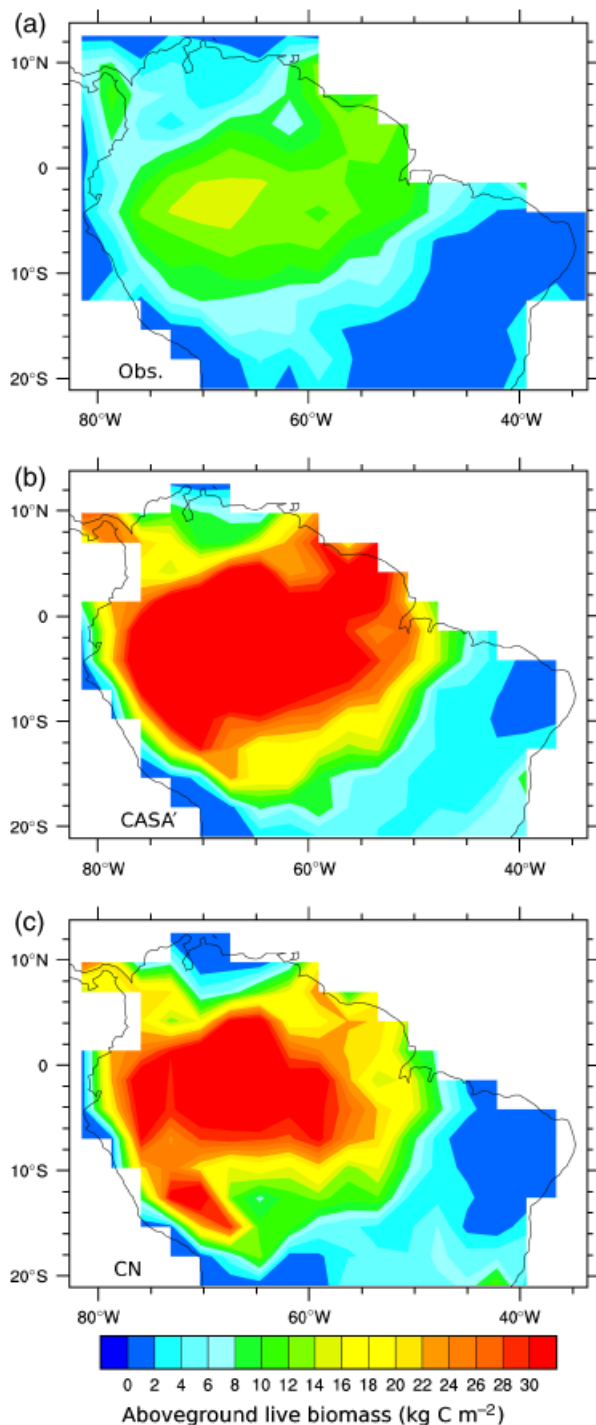


Fig. 5 (a) Aboveground live biomass in the Amazon basin derived using a combination of plot measurements and remote sensing approaches (Saatchi *et al.*, 2007) compared to (b) CASA' and (c) CN model estimates. CASA, Carnegie-Ames-Stanford Approach; CN, carbon-nitrogen.

The CN model estimated the spatial pattern and annual cycle of fire emissions reasonably well in many biomes, including C3 grasslands, tropical savannas, and

tropical forests. The model underestimated the magnitude of contemporary global emissions, however, by a factor of 3. Global CN fire emissions were 0.7 Pg C yr^{-1} during 1997–2004 whereas GFEDv2 estimates were 2.3 Pg C yr^{-1} (Fig. 9). Some of the low model bias here is expected given that the model simulation used in the comparison (experiment 1.4) did not include land use change. Deforestation-linked fires, for example, contribute substantially to contemporary global fire emissions, are sensitive to drought, and have been quantitatively linked to the large increase in the growth rate of atmospheric CO_2 observed during the 1997/1998 El Niño (Page *et al.*, 2002; Van der Werf *et al.*, 2008). Capturing this interannual variability probably also would increase the model's capability to reproduce both the phase and magnitude of interannual variability predicted by TRANSCOM (e.g., Fig. 8).

Our scoring system combined information from different classes of observations with the goal of providing an integrated performance benchmark relevant for climate-carbon simulations (Table 3). We assigned 40% of the score to LAI, NPP, and atmospheric CO_2 annual cycle comparisons. Together, these observations provide an indication of a model's capability to represent contemporary spatial patterns of important ecosystem fluxes and their sensitivity to seasonal variations in climate. We assigned 30% of the score to eddy covariance observations of energy and CO_2 fluxes – recognizing the central role of these data in quantifying a model's ability to represent land surface processes on hourly to interannual time scales. A third set of comparisons accounted for the remaining 30% of the score and were designed to test the transient dynamics of the models on annual to centennial timescales. These include comparisons with biomass inventory observations, FACE experiments, and interannual variability in net ecosystem fluxes and fire emissions. Within individual measurement classes, we gave greater weight to comparisons for which the observations had lower levels of measurement or scaling uncertainty.

Out of 100 possible points, CASA received a score of 65.7 and CN received a score of 58.4. A perfect score probably was not possible given uncertainties associated with scaling several classes of observations and uncertainties in the data products. The different score components, nevertheless, provide a benchmark for gauging model improvement before their use in the IPCC 5th Assessment. Additional work is needed to develop scoring metrics that do not penalize models when model-data differences are within the uncertainty range of the observations. This process will likely require assigning subjective estimates of uncertainties that combine information on measurement precision with other types of error associated with systematic

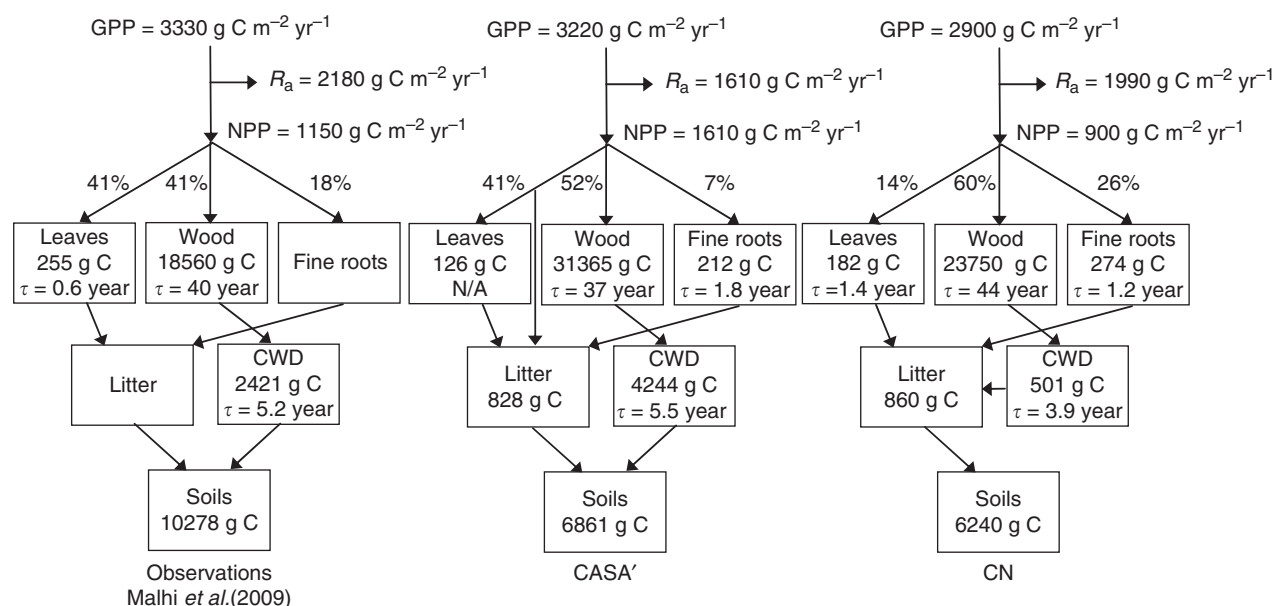


Fig. 6 Carbon pools and fluxes in tropical forests from a synthesis of observations from the Amazon (Malhi *et al.*, 2009) compared with the models.

biases in sampling approaches and scaling requirements.

Discussion

Recommendations for model improvement

The C-LAMP analysis above quantifies strengths and weaknesses in the simulations by two land biogeochemical modules. We present here, as illustrations, how the analysis suggests strategies for model improvement. The strategies may be useful for other land biogeochemical models which share common features and parameterizations with CASA' or CN.

Growing season net flux is the cumulative carbon flux into the land surface during months when GPP exceeds ecosystem respiration and is regulated both by the magnitude of GPP and the phasing of ecosystem respiration relative to GPP. Model estimates of growing season net flux in the northern hemisphere were too low by a factor of 2–3 based on comparison with eddy covariance NEE and the annual cycle of atmospheric CO_2 . As previously discussed, part of this low bias in CN was a result of coupling to a hydrology model that inadequately captured dynamics in frozen soils. Subsequent improvements to the hydrology (Lawrence *et al.*, 2007) increased LAI and NPP in CN in northern regions (after completion of the C-LAMP runs) but only partly improved the low bias in growing season net flux. For both CN and CASA', three additional aspects of the models probably need adjusting – including the repre-

sentation of prognostic LAI, temperature limitation of GPP at low temperatures, and the sensitivity of respiration to temperature.

By shifting the timing of peak LAI in the models from August or September to July as observed in northern ecosystems (Fig. 1), the models may increase carbon uptake during the middle of the growing season, improving agreement with the observations. In temperate forests, there is some evidence that simulated GPP is too high during fall and spring (Fig. 4). After adjusting LAI, additional increases in the low-temperature limitation of photosynthesis may be needed to reduce GPP during these shoulder seasons. Concurrently, reducing the Q_{10} temperature sensitivity of heterotrophic respiration would shift more respiration from mid-summer to fall and spring, further increasing net carbon uptake during the middle part of the growing season. These latter two classes of model adjustment may have important consequences for the strength of the carbon–climate feedback in long-term transient simulations. Both would tend to reduce γ_{L} and $[\gamma_{\text{L}}]$ – the temperature sensitivity of carbon storage on land (Friedlingstein *et al.*, 2006) – and would reduce the gain of the carbon-cycle climate feedback. In this respect, eddy covariance and atmospheric CO_2 observations offer a partial constraint on long term dynamics. A crucial uncertainty remains, however, with respect to whether the temperature sensitivity of longer turnover carbon pools in soils is the same as that of more rapidly cycling pools that contribute to seasonal dynamics (Knorr *et al.*, 2005; Davidson & Janssens, 2006).

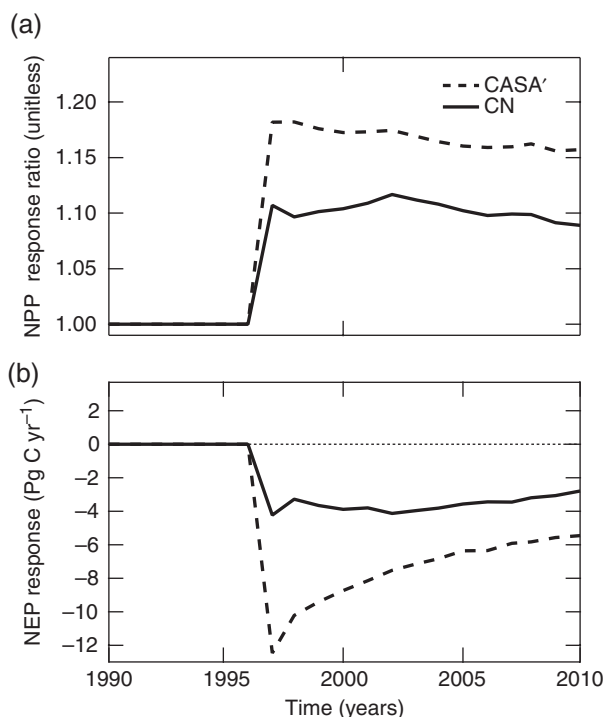


Fig. 7 (a) The response of global NPP to a step change in atmospheric CO₂. Atmospheric CO₂ mixing ratios were increased from 362 ppm in 1996 to 550 ppm in 1997 and thereafter in the models to facilitate comparisons with FACE experiments. The ratio of the elevated CO₂ simulation (exp. 1.6) to the control simulation (exp. 1.5) is shown. (b) Global NEE for the two models in response to the CO₂ step change. NPP, net primary production; NEE, net ecosystem exchange; FACE, free air carbon dioxide enrichment.

Another important deficiency in both models was that woody biomass in tropical forests was too high – by 67–188% for CASA' and by 27–132% for CN based on comparison with syntheses by Malhi *et al.* (2009) and Saatchi *et al.* (2007). In CN, the model has been improved subsequently by changing the dynamic wood allocation algorithm. Wood allocation as a fraction of total biomass allocation was originally treated as a linearly increasing function of annual NPP as observed in global forest NPP datasets (e.g., Cannell, 1982). The Amazon biomass comparison here shows that the extrapolation of this relationship to the highest levels of NPP is not realistic. The CN model was revised to use an approximate linear relationship for low and moderate NPP, but with an asymptote at high NPP limiting the ratio of wood to leaf allocation to 2.3. In CASA', increasing the flow of GPP to autotrophic respiration would improve agreement with the tropical above-ground live biomass measurements. This would also improve model agreement with a recent synthesis of observations that shows autotrophic respiration often exceeds NPP – accounting for $57 \pm 2\%$ (mean ± 1 SE) of GPP when averaged across different forest types (Litton *et al.*, 2007).

The effect of reducing tropical aboveground live biomass on the strength of climate feedbacks is ambiguous. Reducing carbon flow to wood, for example, reduces the sensitivity of carbon storage to CO₂ (β_L) because wood is a long-lived pool that rapidly accumulates carbon in response to stimulation of NPP. As a result of this lower carbon storage capacity, more CO₂ would accumulate in the atmosphere from a given

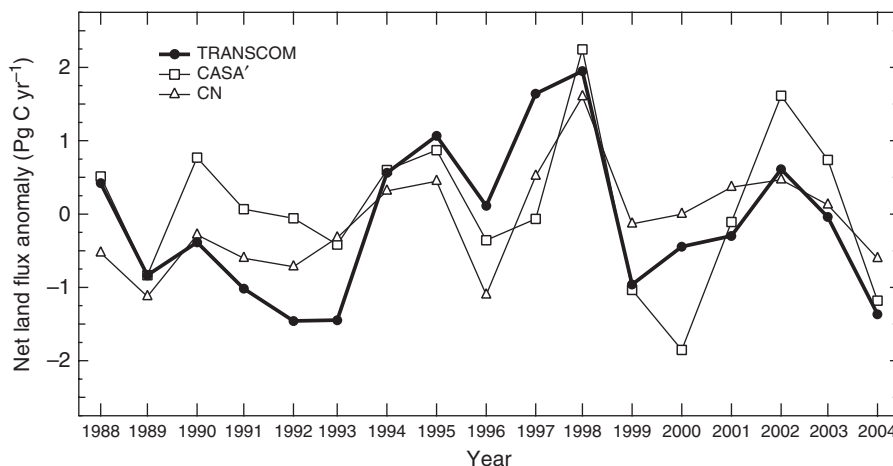


Fig. 8 Interannual variability of the global land flux compared to TRANSKOM atmospheric model inversion estimates. The TRANSKOM fluxes are from Baker *et al.* (2006). These fluxes are the 13-model mean after removing the seasonal cycle and the long-term mean from each model (Baker *et al.*, 2006). The model fluxes are from experiment 1.4. The long-term mean from CASA' and CN during 1991–2000 was removed to enable a direct comparison with the TRANSKOM flux anomalies. CASA, Carnegie-Ames-Stanford Approach; CN, carbon-nitrogen.

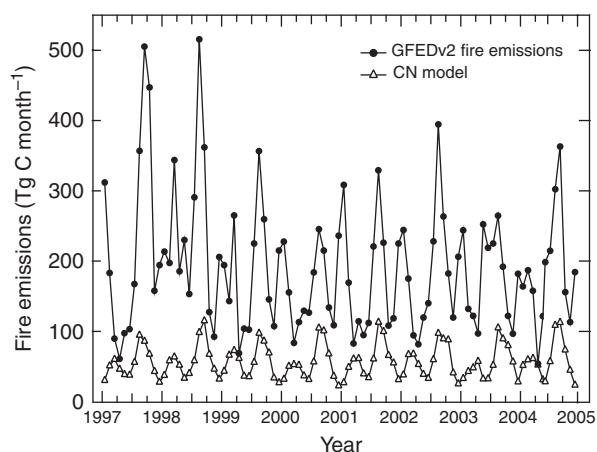


Fig. 9 Global fire emissions from CN compared to the Global Fire Emissions Database version 2 (van der Werf *et al.*, 2006). The version of CASA' analyzed here did not simulate fire emissions. CASA, Carnegie-Ames Stanford Approach; CN, Carbon-nitrogen.

trajectory of fossil fuels—subsequently increasing the gain of the climate–carbon cycle feedback. Smaller tropical forest carbon inventories, however, also may reduce the temperature sensitivity of carbon storage (γ_L) given that climate-driven decreases in NPP were largest in tropical regions in C⁴MIP models (Friedlingstein *et al.*, 2006).

Existing gaps

With our analysis, we have started to build a systematic framework for evaluating land models. Many additional datasets and comparison approaches need to be entrained into this process. Carbon, water, and energy budgets are intrinsically linked. Thus, to better understand issues related to the surface energy budget, satellite observations of albedo (Schaaf *et al.*, 2002), land surface temperature (Wan *et al.*, 2002), net radiation, and evapotranspiration (Cleugh *et al.*, 2007; Mu *et al.*, 2007) need to be integrated within this framework. In parallel, more in depth analysis of the eddy covariance observations are required to more fully exploit the information content of these datasets on hourly to decadal time-scales. To improve the representation of carbon flow within ecosystems, comparison with other types of measurements is necessary, including analysis of existing datasets of leaf litter decomposition (Parton *et al.*, 2007; Zhang *et al.*, 2008), leaf lifespan (Reich *et al.*, 2004), decomposition of coarse woody debris, and turnover of fine roots (e.g., Matamala *et al.*, 2003), as well as soil carbon stocks and radiocarbon estimates of soil carbon turnover times. Regional estimates of aboveground live biomass, including the spatial inventory of North America developed by Blackard *et al.* (2008), have the

potential to constrain mortality and disturbance processes, when combined with measurements of NPP and allocation. A recent synthesis of nitrogen fertilization studies across different biomes (LeBauer & Treseder, 2008) provides a means to test the sensitivity of NPP to changes in nitrogen deposition in CN and other models that include a nitrogen cycle.

Many of the observations described above test model performance at the canopy scale on timescales of hours to decades. Yet many of the models are being used to develop scenarios of future change on timescales of decades to centuries. This poses a challenge for model evaluation. There is emerging recognition, for example, that climate effects on the disturbance regime will be equally important in shaping ecosystems responses as the better understood (and far more extensively studied) effects on canopy level processes such as photosynthesis and decomposition (Running, 2008; Ryan *et al.*, 2008). In this context, available global datasets on burned area should be a priority for future analysis. Few datasets on stand mortality from other forms of disturbance, including insect outbreaks, intense droughts, harvesting and hurricanes (e.g., Chambers *et al.*, 2007) exist in a form that readily allows for comparison with global models, although work is underway to extract some of this information from Landsat imagery for North America (Masek *et al.*, 2008). The paucity of spatial information on these processes slows both model development and evaluation. Development of these datasets and model-data comparisons focused on these processes must be a high priority for the ecological research community.

Another important future step will be to evaluate and report the sensitivity of key ecosystem variables such as GPP, NEE, and fire emissions to temperature and moisture changes. These partial derivatives can be estimated from existing datasets and have the advantage of allowing direct comparison with output from coupled carbon–climate models which may have biases in the representation of the climate system. A first step towards this approach is shown in Fig. 2 where NPP measurements are normalized as a function of precipitation.

Future directions

In past work, the development of biogeochemistry model diagnostics has been done by individual modeling groups as they seek to improve the representation of ecosystem processes within their models. At first, relatively few observations from terrestrial ecosystems were available for model development. In the 1980s and 1990s satellite observations and field experiments such as the First International Satellite Land Surface

Table 3 Summary of model evaluation datasets and analysis

Metric	Metric components	Uncertainty level of obs.	Scaling mismatch	Total score	Sub-score	CASA'	CN
LAI	Matching MODIS observations - Phase (assessed using the month of maximum LAI)	Low	Low	15	6	13.5	12.0
	- Maximum (derived separately for major biome classes)	Moderate	Low		5	4.6	4.3
NPP	- Mean (derived separately for major biome classes) Comparisons with field observations and satellite products	Moderate	Low	10	4	3.8	3.5
	- Matching EMDI Net Primary Production observations	High	High		2	1.5	1.6
	- EMDI comparison, normalized by precipitation	Moderate	Moderate		4	3.0	3.4
	- Correlation with MODIS	High	Low		2	1.6	1.4
	- Latitudinal profile comparison with MODIS	High	Low		2	1.9	1.8
CO ₂ annual cycle	Matching the phase and amplitude at Globalview flask sites 60–90°N	Low	Low	15		10.4	7.7
	30–60°N	Low	Low		6	4.1	2.8
	0–30°N	Moderate	Low		6	4.2	3.2
Energy & CO ₂ fluxes	Matching eddy covariance monthly mean observations			30	3	2.1	1.7
	- Net ecosystem exchange	Low	High		6	2.5	2.1
	- Gross primary production	Moderate	Moderate		6	3.4	3.5
	- Latent heat	Low	Moderate		9	6.4	6.4
	- Sensible heat	Low	Moderate		9	4.9	4.7
Transient dynamics	Evaluating model processes that regulate carbon exchange on decadal to centennial timescales			30		16.7	13.8
	- Aboveground live biomass within the Amazon Basin	Moderate	Moderate		10	5.3	5.0
	- Sensitivity of NPP to elevated levels of CO ₂ ; comparison to temperate forest FACE sites	Low	Moderate		10	7.9	4.1
	- Interannual variability of global carbon fluxes; comparison with TRANSCom	High	Low		5	3.6	3.0
	- Regional and global fire emissions: comparison to GFEDv2	High	Low		5	0.0	1.7
	Total:				100	65.7	58.4

CASA, Carnegie-Ames-Stanford Approach; CN, carbon-nitrogen; NPP, net primary production; FACE, free air carbon dioxide enrichment; MODIS, Moderate Resolution Imaging Spectroradiometer; EMDI, Ecosystem Model Data Intercomparison; LAI, leaf area index; GFEDv2, Global Fire Emissions Database Version 2.

Climatology Project Field Experiment and the Boreal Ecosystem – Atmosphere Study provided key ecosystem-scale observations for land model development. This situation is rapidly evolving with expanding networks of atmospheric and land surface observations, including over 900 site-years of eddy covariance observations from FLUXNET and the development and archiving of multiple datasets from more recent field campaigns such as the Large-Scale Biosphere – Atmosphere Experiment. Model intercomparison projects (MIPs) have used these observations, but often sample them incompletely or using only a subset of available data streams because of time and human resource limitations. The traditional approach has been that modeling teams or intercomparison groups retrieve data sets as needed from existing data centers.

Projection of future changes in ecosystems and their role in climate change is an urgent challenge. The physical climate modeling groups have a successful system where a keystone set of climate model output from IPCC simulations is archived at the Program on Climate Model Diagnosis and Intercomparison center and made available to the community for analysis (Meehl *et al.*, 2007). We argue here that a comparable system is urgently needed for climate–carbon modeling. To start, an important next step is to build a common infrastructure for climate–carbon model-data intercomparison that would extend across different MIPs. This would allow for a more thorough assessment of model uncertainties and would speed model development. It would also stimulate greater interaction between modeling and measurement communities, with the potential for intellectual breakthroughs in both arenas. In the context of future IPCC assessment reports, it would present an objective framework for assessing climate–carbon models and their projections of future changes in the carbon cycle.

The needed infrastructure would have five elements: (1) a series of well-defined model simulation protocols, (2) a common set of variable declarations for model output and data archiving, (3) a coordinated archival system for web-accessing of observations and model output including climate variables, (4) capability to extract information remotely from data centers via autonomous query, and (5) web-accessible software enabling model-data comparison, including the generation of diagnostics and scoring systems for different science objectives. The first three elements have been implemented multiple times in different MIPs, but rarely with standardization that extends across MIPs. The fifth element would require the most human capital – and to succeed internationally would require a well-defined architecture and support from multiple modeling centers.

The advantage of such a system to modeling groups would be that with some investment in simulation and formatting of model output, they would have access to a comprehensive set of diagnostics, the scope of which would be difficult to replicate without considerable effort. For the experimental and observational communities, the comparison process would provide a means for evaluating data quality. Access to multiple model output archives also would provide the measurement community with a quantitative measure of model uncertainty at study sites and would allow for the design of new initiatives and networks that target unconstrained variables or spatial gaps.

Several components of C-LAMP described here may serve as a proto-type for such an intercomparison system (supporting information Fig. S6). A first step at a naming convention for terrestrial biogeochemistry model variables follows that for physical climate models and is available at http://www.climatemodeling.org/c-lamp/protocol/model_output.php. A software package that extracts model output stored with this naming convention, retrieves the corresponding observations, and then generates a series of figures, tables, and cost functions is shown at: http://www.climatemodeling.org/c-lamp/results/diagnostics/CN_vs_CASA/.

Integration of land use change and dynamic vegetation within many of the C⁴MIP models is an important next step for accurately simulating climate–carbon feedbacks (Gitz & Ciais, 2004). As a focus for future model-data intercomparison, output from a land use change MIP may serve as a useful pilot project for developing the software system described above. A crucial science objective would be to understand how biophysical vs. biogeochemical tradeoffs vary with land cover change in different latitude zones (Bala *et al.*, 2007; Bonan, 2008).

Conclusions

To demonstrate a new system for assessing climate–carbon models, we compared two land biogeochemical modules CASA' and CN coupled to CLM using nine different classes of observations (Table 3). Uncertainty levels associated with the different data streams varied considerably. We used information about measurement and scaling uncertainty in a qualitative way to weight the contribution of different data-model comparisons to the overall model score. Both models underestimated the magnitude of carbon uptake during the growing season in northern biomes. In tropical ecosystems, both models overestimated carbon storage in trees. Other model biases included delayed seasonal peak leaf area, too high NPP estimates in CASA', and too low predictions of leaf area and fire emissions by CN. The models

captured some of the interannual variability in the land-atmosphere net CO₂ flux during 1988–2004 based on comparison with TRANSCOM atmospheric CO₂ inversion estimates.

The scoring system we developed attempted to gauge the relevance of different observations for improving model performance with respect to at least two diverging classes of carbon–climate model objectives. These were (1) assessing the strength of the feedback between the carbon cycle and climate system (and thus future emissions requirements for greenhouse gas stabilization) and (2) assessing climate change impacts on ecosystem function.

The evaluation process provides a means for the broader scientific community to gain understanding of the strengths and weaknesses of biogeochemical algorithms. It also provides a benchmark for prioritizing future model improvement and gauging model projections. We propose that a critical next step in this process is for the international community to develop common software and variable protocols that enable data comparison modules to be shared among different MIPs and data centers. This would also allow for more sophisticated model diagnostics tools that could be used to speed model development and to identify data gaps. It would also provide a new approach for critical assessment of observations in the context of other data streams and model results.

Acknowledgements

We thank R. Cook from the Oak Ridge National Laboratory (ORNL) Distributed Active Archive Center and T. Boden from the ORNL Carbon Dioxide Information and Analysis Center for help accessing and interpreting the NPP and Ameriflux observations. We thank Ameriflux colleagues for making the level 4 observations publicly available and NOAA GMD for the atmospheric CO₂ observations. We thank D. Baker for sharing the TRANSCOM interannual flux time series (and for providing updates through 2004) and Y. Malhi for sharing a preprint of his Amazon synthesis paper. This research was partially sponsored by the Climate Change Research Division (CCRD) of the Office of Biological and Environmental Research (OBER) and the Computational Science Research and Partnerships (SciDAC) Division of the Office of Advanced Scientific Computing Research (OASCR) within the US Department of Energy's Office of Science. This research used resources of the National Center for Computational Science at ORNL, which is managed by UT-Battelle, LLC, for the US Department of Energy under Contract No. DE-AC05-00OR22725. Part of this work was performed under auspices of the Office of Science, U.S. Department of Energy, at Lawrence Livermore National Laboratory under Contract No. DE-AC52-07NA27344. The National Center for Atmospheric Research (NCAR) is sponsored by the U.S. National Science Foundation (NSF). Randerson, Mahowald, Doney, and Fung received support from NSF's Carbon and Water Initiative. The Global Fire Emissions Database (GFEDv2) was developed with support from NASA NNG04GK49G.

References

- Ananthakrishnan R, Bernholdt DE, Bharathi S *et al.* (2007) Building a global federation system for climate change research: the earth system grid center for enabling technologies (ESG-CET). *Journal of Physics: Conference Series*, **78**, 012050.
- Baker DF, Law RM, Gurney KR *et al.* (2006) TransCom 3 inversion intercomparison: impact of transport model errors on the interannual variability of regional CO₂ fluxes, 1988–2003. *Global Biogeochemical Cycles*, **20**, GB1002, doi: 10.1029/2004GB002439.
- Bala G, Caldeira K, Wickett M, Phillips TJ, Lobell DB, Delire C, Mirin A (2007) Combined climate and carbon-cycle effects of large-scale deforestation. *Proceedings of the National Academy of Sciences of the United States of America*, **104**, 6550–6555.
- Barford CC, Wofsy SC, Goulden ML *et al.* (2001) Factors controlling long- and short-term sequestration of atmospheric CO₂ in a mid-latitude forest. *Science*, **294**, 1688–1691.
- Barker T, Bashmakov I, Bernstein L *et al.* (2007) Technical summary. In: *Climate Change 2007: Mitigation. Contribution of Working Group III to the Fourth Assessment Report of the Intergovernmental Panel on Climate Change* (eds Metz B, Davidson OR, Bosch PR, Dave R, Meyer LA), pp. 25–94. Cambridge University Press, UK and New York, NY, USA.
- Bernholdt D, Bharathi S, Brown D *et al.* (2005) The Earth System Grid: supporting the next generation of climate modeling research. *Proceedings of the IEEE*, **90**, 485–495, doi: 10.1109/JPROC.2004.842745.
- Berthelot M, Friedlingstein P, Ciais P, Monfray P, Dufresne JL, Le Treut H, Fairhead L (2002) Global response of the terrestrial biosphere to CO₂ and climate change using a coupled climate-carbon cycle model. *Global Biogeochemical Cycles*, **16**, 1084, doi: 10.1029/2001GB001827.
- Betts RA, Cox PM, Collins M, Harris PP, Huntingford C, Jones CD (2004) The role of ecosystem–atmosphere interactions in simulated Amazonian precipitation decrease and forest dieback under global climate warming. *Theoretical and Applied Climatology*, **78**, 157–175.
- Blackard JA, Finco MV, Helmer EH *et al.* (2008) Mapping U.S. forest biomass using nationwide forest inventory data and moderate resolution information. *Remote Sensing of Environment*, **112**, 1658–1677.
- Bonan GB (2008) Forests and climate change: forcings, feedbacks, and the climate benefits of forests. *Science*, **320**, 1444–1449.
- Cannell MGR (1982) *World Forest Biomass and Primary Production Data*. Academic Press, London.
- Chambers JQ, Fisher JL, Zeng HC, Chapman EL, Baker DB, Hurtt GC (2007) Hurricane Katrina's carbon footprint on U.S. Gulf Coast forests. *Science*, **318**, 1107–1107.
- Cleugh HA, Leuning R, Mu QZ, Running SW (2007) Regional evaporation estimates from flux tower and MODIS satellite data. *Remote Sensing of Environment*, **106**, 285–304.
- Conway TJ, Tans PP, Waterman LS, Thoning KW (1994) Evidence for interannual variability of the carbon-cycle from the National-Oceanic-and-Atmospheric-Administration Climate-Monitoring-and-Diagnostics-Laboratory Global-Air-Sampling-Network. *Journal of Geophysical Research-Atmospheres*, **99**, 22831–22855.

- Cox PM, Betts RA, Collins M, Harris PP, Huntingford C, Jones CD (2004) Amazonian forest dieback under climate–carbon cycle projections for the 21st century. *Theoretical and Applied Climatology*, **78**, 137–156.
- Cox PM, Betts RA, Jones CD, Spall SA, Totterdell IJ (2000) Acceleration of global warming due to carbon-cycle feedbacks in a coupled climate model. *Nature*, **408**, 184–187.
- Cramer W, Bondeau A, Woodward FI *et al.* (2001) Global response of terrestrial ecosystem structure and function to CO₂ and climate change: results from six dynamic global vegetation models. *Global Change Biology*, **7**, 357–373.
- Crisp D, Atlas RM, Breon FM *et al.* (2004) The orbiting carbon observatory (OCO) mission. *Advances in Space Research*, **34**, 700–709.
- Dargaville RJ, Heimann M, McGuire AD *et al.* (2002) Evaluation of terrestrial carbon cycle models with atmospheric CO₂ measurements: results from transient simulations considering increasing CO₂, climate, and land-use effects. *Global Biogeochemical Cycles*, **16**, 1092, doi: 10.1029/2001GB001426.
- Davidson EA, Janssens IA (2006) Temperature sensitivity of soil carbon decomposition and feedbacks to climate change. *Nature*, **440**, 165–173.
- Denman KL, Brasseur G, Chidthaisong A *et al.* (2007) Couplings between changes in the climate system and biogeochemistry. In: *Contribution of Working Group I to the Fourth Assessment Report of the Intergovernmental Panel on Climate Change* (eds Solomon S, Qin D, Manning M *et al.*), pp. 499–588. Cambridge University Press, Cambridge, UK and New York, NY, USA.
- Desai AR, Bolstad PV, Cook BD *et al.* (2005) Comparing net ecosystem exchange of carbon dioxide between an old-growth and mature forest in the upper Midwest, USA. *Agricultural and Forest Meteorology*, **128**, 33–55.
- Dickinson RE, Oleson KW, Bonan G *et al.* (2006) The Community Land Model and its climate statistics as a component of the Community Climate System Model. *Journal of Climate*, **19**, 2302–2324.
- Dickinson RE, Shaikh M, Bryant R, Graumlich L (1998) Interactive canopies for a climate model. *Journal of Climate*, **11**, 2823–2836.
- Doney SC, Lindsay K, Fung IY, John J (2006) Natural variability in a stable, 1000-yr global coupled climate–carbon cycle simulation. *Journal of Climate*, **19**, 3033–3054.
- Eaton B, Gregory J, Drach B *et al.* (2008) *NetCDF Climate and Forecast (CF) metadata conventions. Technical Specifications Version 1.3, Program for Climate Model Diagnosis and Intercomparison report*. Available at: <http://cf-pcmdi.llnl.gov/documents/cf-conventions> (72 pp) (accessed 12 July 2008).
- Falge E, Baldocchi D, Tenhunen J *et al.* (2002) Seasonality of ecosystem respiration and gross primary production as derived from FLUXNET measurements. *Agricultural and Forest Meteorology*, **113**, 53–74.
- Fearnside PM (1992) Forest biomass in Brazilian Amazonia – Comment. *Interciencia*, **17**, 19–27.
- Feddema J, Oleson K, Bonan G, Mearns L, Washington W, Meehl G, Nychka D (2005) A comparison of a GCM response to historical anthropogenic land cover change and model sensitivity to uncertainty in present-day land cover representations. *Climate Dynamics*, **25**, 581–609.
- Field CB, Lobell DB, Peters HA, Chiariello NR (2007) Feedbacks of terrestrial ecosystems to climate change. *Annual Review of Environment and Resources*, **32**, 1–29.
- Figueira AMES, Miller SD, de Sousa CAD *et al.* (2008) Effects of selective logging on tropical forest tree growth. *Journal of Geophysical Research - Biogeosciences*, **113**, G00B05, doi: 10.1029/2007JG000577.
- Friedlingstein P, Bopp L, Ciais P *et al.* (2001) Positive feedback between future climate change and the carbon cycle. *Geophysical Research Letters*, **28**, 1543–1546.
- Friedlingstein P, Cox P, Betts R *et al.* (2006) Climate–carbon cycle feedback analysis: results from the (CMIP)-M-4 model inter-comparison. *Journal of Climate*, **19**, 3337–3353.
- Friedlingstein P, Dufresne JL, Cox PM, Rayner P (2003) How positive is the feedback between climate change and the carbon cycle? *Tellus Series B – Chemical and Physical Meteorology*, **55**, 692–700.
- Friedlingstein P, Joel G, Field CB, Fung IY (1999) Toward an allocation scheme for global terrestrial carbon models. *Global Change Biology*, **5**, 755–770.
- Fung IY, Doney SC, Lindsay K, John J (2005) Evolution of carbon sinks in a changing climate. *Proceedings of the National Academy of Sciences of the United States of America*, **102**, 11201–11206.
- Giglio L, van der Werf GR, Randerson JT, Collatz GJ, Kasibhatla P (2006) Global estimation of burned area using MODIS active fire observations. *Atmospheric Chemistry and Physics*, **6**, 957–974.
- Gitz V, Ciais P (2004) Future expansion of agriculture and pasture acts to amplify atmospheric CO₂ levels in response to fossil-fuel and land-use change emissions. *Climatic Change*, **67**, 161–184.
- Gurney KR, Law RM, Denning AS *et al.* (2004) Transcom 3 inversion intercomparison: model mean results for the estimation of seasonal carbon sources and sinks. *Global Biogeochemical Cycles*, **18**, GB1010, doi: 10.1029/2003GB002111.
- Heimann M, Esser G, Haxeltine A *et al.* (1998) Evaluation of terrestrial carbon cycle models through simulations of the seasonal cycle of atmospheric CO₂: first results of a model intercomparison study. *Global Biogeochemical Cycles*, **12**, 1–24.
- Heinsch FA, Reeves M, Votava P *et al.* (2003) *User's Guide GPP and NPP (MOD17A2/A3) Products NASA MODIS Land Algorithm. Version 2.0*. University of Montana, Missoula, MT.
- Heinsch FA, Zhao MS, Running SW *et al.* (2006) Evaluation of remote sensing based terrestrial productivity from MODIS using regional tower eddy flux network observations. *IEEE Transactions on Geoscience and Remote Sensing*, **44**, 1908–1925.
- Hickler T, Smith B, Prentice IC, Mjöfors K, Miller P, Arneth A, Sykes MT (2008) CO₂ fertilization in temperate FACE experiments not representative of boreal and tropical forests. *Global Change Biology*, **14**, 1531–1542.
- Hoffman FM, Randerson JT, Fung IY *et al.* (2008) The carbon-land model intercomparison project (C-LAMP): a protocol and evaluation metrics for global terrestrial biogeochemistry models. In: *International Congress on Environmental Modeling and Software 4th Biennial Meeting on Integrating Science and Information Technology for Environmental Assessment and Decision Making* (eds Sanchez-Marre M, Begar J, Comas J, Rizzoli A, Guariso G), International Environmental Modelling and Software Society, Barcelona, Spain.

- Houghton RA, Lawrence KT, Hackler JL, Brown S (2001) The spatial distribution of forest biomass in the Brazilian Amazon: a comparison of estimates. *Global Change Biology*, **7**, 731–746.
- Hurtt GC, Frolking S, Fearon MG *et al.* (2006) The underpinnings of land-use history: three centuries of global gridded land-use transitions, wood-harvest activity, and resulting secondary lands. *Global Change Biology*, **12**, 1208–1229.
- Kaminski T, Knorr W, Rayner PJ, Heimann M (2002) Assimilating atmospheric data into a terrestrial biosphere model: a case study of the seasonal cycle. *Global Biogeochemical Cycles*, **16**, 1066, doi: 10.1029/2001GB001463.
- Knorr W, Prentice IC, House JI, Holland EA (2005) Long-term sensitivity of soil carbon turnover to warming. *Nature*, **433**, 298–301.
- Lamarque JF, Kiehl JT, Brasseur GP *et al.* (2005) Assessing future nitrogen deposition and carbon cycle feedback using a multi-model approach: analysis of nitrogen deposition. *Journal of Geophysical Research–Atmospheres*, **110**, Art. No. D19303. doi: 10.1029/2005JD005825.
- Lawrence DM, Thornton PE, Oleson KW, Bonan GB (2007) The partitioning of evapotranspiration into transpiration, soil evaporation, and canopy evaporation in a GCM: impacts on land–atmosphere interaction. *Journal of Hydrometeorology*, **8**, 862–880.
- LeBauer DS, Treseder KK (2008) Nitrogen limitation of net primary production in terrestrial ecosystems is globally distributed. *Ecology*, **89**, 371–379.
- Litton CM, Raich JW, Ryan MG (2007) Carbon allocation in forest ecosystems. *Global Change Biology*, **13**, 2089–2109.
- Malhi Y, Aragao LEOC, Metcalfe DB *et al.* (2009) Comprehensive assessment of carbon productivity, allocation, and storage in three Amazonian forests. *Global Change Biology*, doi: 10.1111/j.1365-2486.2008.01780.x.
- Masarie KA, Tans PP (1995) Extension and integration of atmospheric carbon-dioxide data into a globally consistent measurement record. *Journal of Geophysical Research–Atmospheres*, **100**, 11593–11610.
- Masek JG, Huang C, Wolfe R, Cohen W, Hall F, Kutler J, Nelson P (2008) North American forest disturbance mapped from a decadal Landsat record. *Remote Sensing of Environment*, **112**, 2914–2926.
- Matamala R, Gonzalez-Meler MA, Jastrow JD, Norby RJ, Schlesinger WH (2003) Impacts of fine root turnover on forest NPP and soil C sequestration potential. *Science*, **302**, 1385–1387.
- Matthews HD (2007) Implications of CO₂ fertilization for future climate change in a coupled climate–carbon model. *Global Change Biology*, **13**, 1068–1078.
- Matthews HD, Eby M, Ewen T, Friedlingstein P, Hawkins BJ (2007) What determines the magnitude of carbon cycle–climate feedbacks? *Global Biogeochemical Cycles*, **21**, GB2012, doi: 10.1029/2006GB002733.
- McGuire AD, Sitch S, Clein JS *et al.* (2001) Carbon balance of the terrestrial biosphere in the twentieth century: analyses of CO₂, climate and land use effects with four process-based ecosystem models. *Global Biogeochemical Cycles*, **15**, 183–206.
- Meehl GA, Covey C, Delworth T *et al.* (2007) The WCRP CMIP3 multimodel dataset: a new era in climate change research. *Bulletin of the American Meteorological Society*, **88**, 1383–1394.
- Miller SD, Goulden ML, Menton MC, da Rocha HR, de Freitas HC, Figueira A, de Sousa CAD (2004) Biometric and micro-meteorological measurements of tropical forest carbon balance. *Ecological Applications*, **14**, S114–S126.
- Morales P, Sykes MT, Prentice IC *et al.* (2005) Comparing and evaluating process-based ecosystem model predictions of carbon and water fluxes in major European forest biomes. *Global Change Biology*, **11**, 2211–2233.
- Mu Q, Heinsch FA, Zhao M, Running SW (2007) Development of a global evapotranspiration algorithm based on MODIS and global meteorology data. *Remote Sensing of Environment*, **111**, 519–536.
- Myneni RB, Hoffman S, Knyazikhin Y *et al.* (2002) Global products of vegetation leaf area and fraction absorbed PAR from year one of MODIS data. *Remote Sensing of Environment*, **83**, 214–231.
- Nevison CD, Mahowald NM, Doney SC *et al.* (2008) Contribution of ocean, fossil fuel, land biosphere and biomass burning carbon fluxes to seasonal and interannual variability in atmospheric CO₂. *Journal of Geophysical Research – Biogeoscience*, **113**, G01010, doi: 10.1029/2007JG000408.
- Norby RJ, DeLucia EH, Gielen B *et al.* (2005) Forest response to elevated CO₂ is conserved across a broad range of productivity. *Proceedings of the National Academy of Sciences of the United States of America*, **102**, 18052–18056.
- Oleson KW, Niu GY, Yang ZL *et al.* (2008) Improvements to the Community Land Model and their impact on the hydrological cycle. *Journal of Geophysical Research–Biogeosciences*, **113**, G01021, doi: 10.1029/2007JG000563.
- Olson RJ, Scurlock JMO, Prince SD, Zheng DL, Johnson KR (2001) NPP Multi-Biome: NPP and Driver Data for Ecosystem Model-Data Intercomparison. Available on-line [http://www.daac.ornl.gov] from the Oak Ridge National Laboratory Distributed Active Archive Center, Oak Ridge, Tennessee, USA.
- Page SE, Siebert F, Rieley JO, Boehm HDV, Jaya A, Limin S (2002) The amount of carbon released from peat and forest fires in Indonesia during 1997. *Nature*, **420**, 61–65.
- Parton W, Silver WL, Burke IC *et al.* (2007) Global-scale similarities in nitrogen release patterns during long-term decomposition. *Science*, **315**, 361–364.
- Potter CS, Randerson JT, Field CB, Matson PA, Vitousek PM, Mooney HA, Klooster SA (1993) Terrestrial ecosystem production – a process model based on global satellite and surface data. *Global Biogeochemical Cycles*, **7**, 811–841.
- Qian TT, Dai AG, Trenberth KE, Oleson KW (2006) Simulation of global land surface conditions from 1948 to 2004. Part I: forcing data and evaluations. *Journal of Hydrometeorology*, **7**, 953–975.
- Randerson JT, Still CJ, Balle JJ *et al.* (2002) Carbon isotope discrimination of arctic and boreal biomes inferred from remote atmospheric measurements and a biosphere–atmosphere model. *Global Biogeochemical Cycles*, **16**, 1028, doi:10.1029/2001GB001435.
- Randerson JT, Thompson MV, Conway TJ, Fung IY, Field CB (1997) The contribution of terrestrial sources and sinks to trends in the seasonal cycle of atmospheric carbon dioxide. *Global Biogeochemical Cycles*, **11**, 535–560.

- Reich PB, Uhl C, Walters MB, Prugh L, Ellsworth DS (2004) Leaf demography and phenology in Amazonian rain forest: a census of 40 000 leaves of 23 tree species. *Ecological Monographs*, **74**, 3–23.
- Running SW (2008) Climate change – ecosystem disturbance, carbon, and climate. *Science*, **321**, 652–653.
- Ryan M, Archer S, Birdsey R *et al.* (2008) Land resources. In: *The Effects of Climate Change on Agriculture, Land Resources, Water Resources, and Biodiversity. A Report by the US Climate Change Science Program and the Subcommittee on Global Change Research*, pp. 75–120. US Department of Agriculture, Washington, DC, USA.
- Saatchi SS, Houghton RA, Alvala R, Soares JV, Yu Y (2007) Distribution of aboveground live biomass in the Amazon basin. *Global Change Biology*, **13**, 816–837.
- Schaaf CB, Gao F, Strahler AH *et al.* (2002) First operational BRDF, albedo nadir reflectance products from MODIS. *Remote Sensing of Environment*, **83**, 135–148.
- Schimel DS, Emanuel W, Rizzo B *et al.* (1997) Continental scale variability in ecosystem processes: models, data, and the role of disturbance. *Ecological Monographs*, **67**, 251–271.
- Stephens BB, Gurney KR, Tans PP *et al.* (2007) Weak northern and strong tropical land carbon uptake from vertical profiles of atmospheric CO₂. *Science*, **316**, 1732–1735.
- Stockli R, Lawrence DM, Niu GY *et al.* (2008) Use of FLUXNET in the community land model development. *Journal of Geophysical Research–Biogeosciences*, **113**, G01025, doi: 10.1029/2007jg000562.
- Thonicke K, Venevsky S, Sitch S, Cramer W (2001) The role of fire disturbance for global vegetation dynamics: coupling fire into a Dynamic Global Vegetation Model. *Global Ecology and Biogeography*, **10**, 661–677.
- Thornton PE, Lamarque JF, Rosenbloom NA, Mahowald NM (2007) Influence of carbon-nitrogen cycle coupling on land model response to CO₂ fertilization and climate variability. *Global Biogeochemical Cycles*, **21**, GB4018, doi: 10.1029/2006GB002868.
- Thornton PE, Law BE, Gholz HL *et al.* (2002) Modeling and measuring the effects of disturbance history and climate on carbon and water budgets in evergreen needleleaf forests. *Agricultural and Forest Meteorology*, **113**, 185–222.
- Thornton PE, Rosenbloom NA (2005) Ecosystem model spin-up: estimating steady state conditions in a coupled terrestrial carbon and nitrogen cycle model. *Ecological Modelling*, **189**, 25–48.
- Thornton PE, Zimmermann NE (2007) An improved canopy integration scheme for a land surface model with prognostic canopy structure. *Journal of Climate*, **20**, 3902–3923.
- van der Werf GR, Dempewolf J, Trigg SN *et al.* (2008) Climate regulation of fire emissions and deforestation in equatorial Asia. *Proceedings of the National Academy of Sciences of the United States of America*, **105**, 20350–20355, doi:10.1073/pnas.0803375105.
- van der Werf GR, Randerson JT, Giglio L, Collatz GJ, Kasibhatla PS, Arellano AF (2006) Interannual variability in global biomass burning emissions from 1997 to 2004. *Atmospheric Chemistry and Physics*, **6**, 3423–3441.
- Vieira S, de Camargo PB, Selhorst D *et al.* (2004) Forest structure and carbon dynamics in Amazonian tropical rain forests. *Oecologia*, **140**, 468–479.
- Wan ZM, Zhang YL, Zhang QC, Li ZL (2002) Validation of the land-surface temperature products retrieved from Terra Moderate Resolution Imaging Spectroradiometer data. *Remote Sensing of Environment*, **83**, 163–180.
- Wilson KB, Baldocchi DD (2001) Comparing independent estimates of carbon dioxide exchange over 5 years at a deciduous forest in the southeastern United States. *Journal of Geophysical Research – Atmospheres*, **106**, 34167–34178.
- Yang Z, Washenfelder RA, Keppel-Aleks G *et al.* (2007) New constraints on Northern Hemisphere growing season net flux. *Geophysical Research Letters*, **34**, L12807, doi: 10.1029/2007GL029742.
- Zhang D, Hui D, Luo Y, Zhou G (2008) Rates of litter decomposition in terrestrial ecosystems: global patterns and controlling factors. *Journal of Plant Ecology*, **1**, 85–93, doi: 10.1093/jpe/rtn1002.
- Zhao M, Running SW, Nemani RR (2006) Sensitivity of Moderate Resolution Imaging Spectroradiometer (MODIS) terrestrial primary production to the accuracy of meteorological reanalyses. *Journal of Geophysical Research – Biogeosciences*, **111**, G01002, doi: 10.1029/2004JG000004.
- Zhao MS, Heinsch FA, Nemani RR, Running SW (2005) Improvements of the MODIS terrestrial gross and net primary production global data set. *Remote Sensing of Environment*, **95**, 164–176.

Supporting Information

Additional Supporting Information may be found in the online version of this article:

Figure S1. Conceptual diagram of observations available for testing carbon-climate models. Ice core measurements of the atmospheric CO₂ record provide constraints on the sum of ocean and land carbon fluxes when this information is combined with fossil fuel inventory time series. Isotope measurements from ice cores allow for similar constraints but including gross exchanges and reservoir turnover times. Contemporary atmospheric CO₂ observations from flask networks (NOAA GMD) and satellites (e.g., the Orbiting Carbon Observatory) provide information about the seasonal dynamics of net ecosystem exchange and continental-scale fluxes on timescales of years to decades. Biomass inventories are sparse but crucial for constraining allocation, tree mortality, and the mass of carbon vulnerable to deforestation. Satellite observations of leaf area index and other ecosystem variables provide global coverage at a high temporal resolution for a period of almost three decades, although cross-platform calibrations introduce considerable uncertainty. Free-Air Carbon dioxide Enrichment (FACE) experiments have quantified elevated CO₂ effects on ecosystem processes in temperate ecosystems, but less information exists for tropical forest and boreal biomes that account for most of terrestrial GPP and aboveground carbon storage.

Figure S2. Comparison of net primary production for a) CASA' and b) CN models with class A observations from the Ecosystem Model Data Intercomparison Initiative (EMDI). The same comparison for class B observations is shown in c) and d).

Figure S3. Zonal mean net primary production from MODIS satellite-based estimates compared with the models. We used the MOD17A3 collection 4.5 product from MODIS for this comparison (Heinsch *et al.*, 2003). We show the 200–2004 zonal mean and compare this model experiment 1.4 during the same period.

Figure S4. The zonal mean response of NPP to a step change in atmospheric CO₂ following the FACE experimental protocol. The model NPP response was averaged over the first 5 years after enrichment.

Figure S5. a) The global net land flux from experiment 1.4. This simulation includes climate variability and time-varying atmospheric CO₂ and nitrogen deposition. Climate for a 25-year span (1948–1972) was cycled until 1948, the beginning of the NCAR/NCEP reanalysis period. b) The difference in flux between experiments 1.4 and the climate only simulation (experiment 1.3). This panel shows the fluxes caused solely from the atmospheric CO₂ and nitrogen deposition forcing. c) The land flux driven solely by climate (experiment 1.3) during 1973–2004.

Figure S6. Conceptual diagram showing how a climate ecosystem data-model intercomparison system (CEDMIS) might function in the context of existing data centers and model archiving capabilities. CEDMIS would extract information from archived data sets and models to generate intercomparison diagnostics, using a series of scoring, visualization, and data extraction software tools. A key goal would be make the intercomparison diagnostics into modules that could be reused in multiple model-intercomparison projects (MIPs) in an open source format. This system could be used in a stand alone mode for individual model development or as the basis for community wide MIPs. Key data sources would include the Carbon Dioxide Information and Analysis Center (CDIAC), NASA's Oak Ridge National Lab (ORNL) and Land Processes (LP) Distributed Active Archiving Centers (DAACs), NOAA's Global Monitoring Division trace gas archives (including retrieved fluxes by means of atmospheric inversions such as TRANSCOM and CarbonTracker), and NSF's Long Term Ecological Research (LTER).

Please note: Wiley-Blackwell are not responsible for the content or functionality of any supporting materials supplied by the authors. Any queries (other than missing material) should be directed to the corresponding author for the article.